①

RF Monolithics
4441 Sigma Rd.
Dallas, Texas 75244
Contract # DAAL01 - 87 - C - 0731
January 29, 1988

SURFACE ACOUSTIC WAVE BAND ELIMINATION FILTER

Phase I Final Report

Report Prepared By: Michael B. King and Jeffrey C. Andle

DTIC
ELECTE
APR 2 4 1989
S H D

"The view, opinions, and/or findings contained in this report are those of the authors and should not be construed as an official Department of the Army position, policy, or decision, unless designated by other documentation."

89

I. INTRODUCTION

1.1 BACKGROUND

SAW devices are monolithic signal processing elements for frequencies between 10 MHz and 2000 MHz. SAW devices have many performance advantages which have resulted in wide ranging applications in military, commercial, and consumer systems. However, it has been generally recognized that SAW technology has been limited to bandpass filter functions and further that these filters typically have very high insertion loss (typically greater than 20 dB).

There are at least three more classes of filter functions that are desirable, specifically, bandstop filters, highpass filters, and lowpass filters. This research program extends SAW technology to cover the first of these three classes and furthermore accomplishes the bandstop filtering function with very low insertion loss and very high passband power handling capability.

While conventional SAW filters have many advantages over the existing LC (inductor-capacitor) technologies, their high insertion loss and limited power handling capability have often prevented SAW filters from being used to replace LC filters.

For example, receiver front end filters have traditionally not been implemented with SAW filter technology because of the high insertion loss and the associated degradation of sensitivity. Prototypes of the SAW notch filter which are being developed under this program have already demonstrated insertion loss of less than 2dB. This notch filter could be very useful for eliminating specific interfering signals at a receiver front end without degrading sensitivity.

SAW devices have never been used as transmitter filters because of their high insertion loss and low power handling capabilities. However, modern mission requirements for co-located multiple transmitters and receivers in military environments require that the output signals from transmitters

be free from spurious signals. This recently developed notch filter has the power handling and loss capabilities that are consistant with transmitter output filtering needs. Initial experiments on prototype filters at 1030 MHz indicated in excess of 5W power handling capability out of band. Further improvements appear readily attainable.

LC notch filters have been available for many years in the UHF range. They have been used sparingly since the low Q generally results in very poor skirt selectivity. The high performance notch filters described in this report are the result of research into methods for using the inherently high Q of SAW devices for notch filters. / /

1.2 PREVIOUS SAW NOTCH FILTERS

The earliest approach to SAW notch filters attempted to implement the notch using the traditional transversal structure with either a grating between two extremely wideband transducers, or by transducer weighting. Since useable notch filters must have large bandwidth, and since SAW devices have extremely high insertion loss at broad bandwidths, this approach is not desirable.

More recently, Koyomada[1] has demonstrated that a SAW transducer could be used as an admittance element in the classical bridged-T all-pass circuit. This allows a broad passband, since the energy is not propagated through the SAW. This was accomplished by using the one-port transducer as a capacitor in the circuit. The inband radiation conductance of the SAW device was used to selectively decrease the Q of the capacitor at the resonant frequency, causing the circuit to attenuate frequencies near the SAW resonance. Although this was a significant advance in the technology of SAW notch filters, the resulting performance was not acceptable for practical band-elimination filters.

Koyomada's filter was impractical since the width of the

notch was less than the temperature drift of the filter. The stopband width was 390 parts per million (ppm) on lithium niobate while the notch frequency would drift 15,000 ppm (1.5%) over the MIL SPEC temperature range. Koyomada also demonstrated a quartz notch with a 90 ppm notch width. However, most quartz SAW transducers have a center frequency drift of 300 ppm over the MIL environment range.

Also, the shape factor of Koyomada's notch filter was poor. The shape factor on either substrate was approximately 50:1 (1dB : 40dB).

1.3 RFM SAW NOTCH ELEMENT (SNE)

RF Monolithics has invested a significant amount of its resources into SAW notch filter technology. This research led to the development of a unique SAW Notch Element (SNE). This patented structure offers both wider stopbands and better shape factor than either conventional LC notch filters or previous SAW notch filters[2]. A major portion of the reported effort was placed on the development of a rigorous model of the SNE.

The SNE (SAW Notch Element) is a one-port admittance (or impedance) element having essentially constant conductance and susceptance near its center frequency. The frequency band over which this is true is referred to as the "flatband" and helps to obtain both wider notches and improved shape factor. This element is usually implemented using essentially unweighted transducers on specific orientations of common SAW substrates.

The improved shape factor is achieved by tailoring the radiation conductance and susceptance to the more optimal shape described above. **Figure 1.1** shows the characteristics of an ideal notch impedance element. Note that both conductance and susceptance are constant across the desired stopband, while immediately outside the stopband, the conductance is zero and the susceptance appears to be that of a capacitor. However, such an ideal impedance element is physically impossible, due to the Hilbert transform relationship between the conductance and
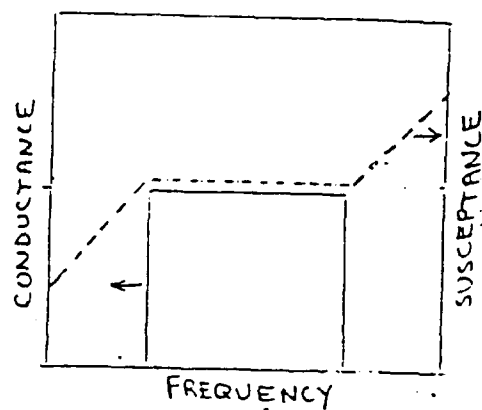
Figure 1.1 Ideal
Notch Element

Figure 1.2 Practical
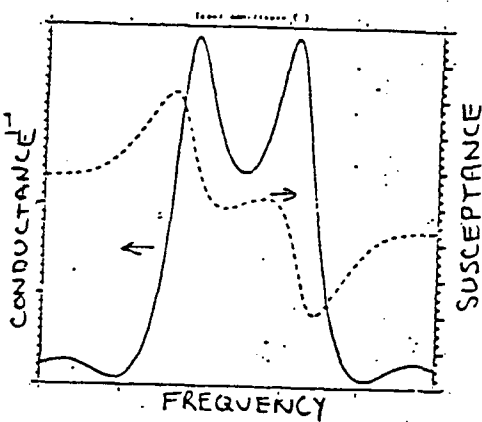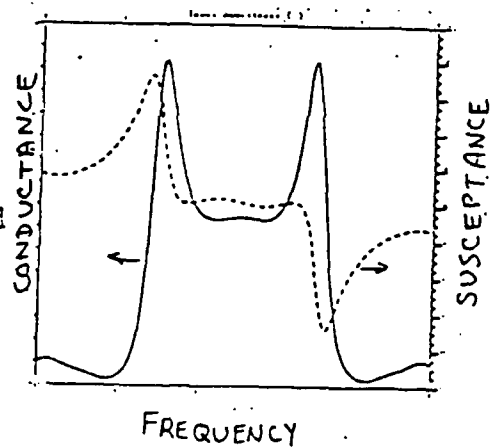SAW Notch Element
(SNE)

Figure 1.3 Improved
Saw Notch Element
(SNE)

susceptance of any causal circuit element[3].

It can be shown that for the SNE to have flat susceptance in the stopband and be capacitive in the passband, it is necessary for the conductance to be "concave up" around the stopband[2]. A practical SAW realization of this admittance is shown in **Figure** 1.2. The twin peaks of the conductance are a natural phenomenon of a normal SAW transducer having internal reflections on certain orientations of common SAW substrates.

Figure 1.3 shows a further improvement on the impedance element resulting from the use of a moderate weighting function and the addition of weak reflective gratings.

Another important advantage of the RFM SNE is its ability to implement notch filters with stopbands significantly wider than the temperature drift. For example, RFM has demonstrated a 1030 MHz quartz notch with a 20 dB width of 14 MHz. The temperature drift of this notch is only 300 kHz.

1.4 NOTCH FILTER CIRCUITS

Recently RF Monolithics has demonstrated two different notch filter circuits which are capable of broad passbands, low passband loss, good notch depth, and low shape factor. The first of these circuits ,shown in **Figure** 1.4, uses the SNE to replace the capacitors in an improved "bridged-T" circuit[4]. The second, shown in **Figure** 1.5, uses the SNE as a termination element for a reflective quadrature hybrid notch circuit.

One example of a practical application of the bridged-T circuit is for a CATV descrambling system. **Figure 1.6** shows the response of a prototype circuit for this application. The filter exhibits a passband loss less than 2 dB from DC to above 1 GHz. The notch width is 70 kHz at the 40 dB points, obtaining a fractional bandwidth of .035%. This is more than adequate to cover the 20 kHz of temperature drift exhibited by this cut of quartz over the desired operating temperature range of -40°C to $+60^{o}$C. This notch achieves a tenfold improvement in shape factor over the presently used LC notch.

Figure 1.4 Improved - Bridged - T Notch
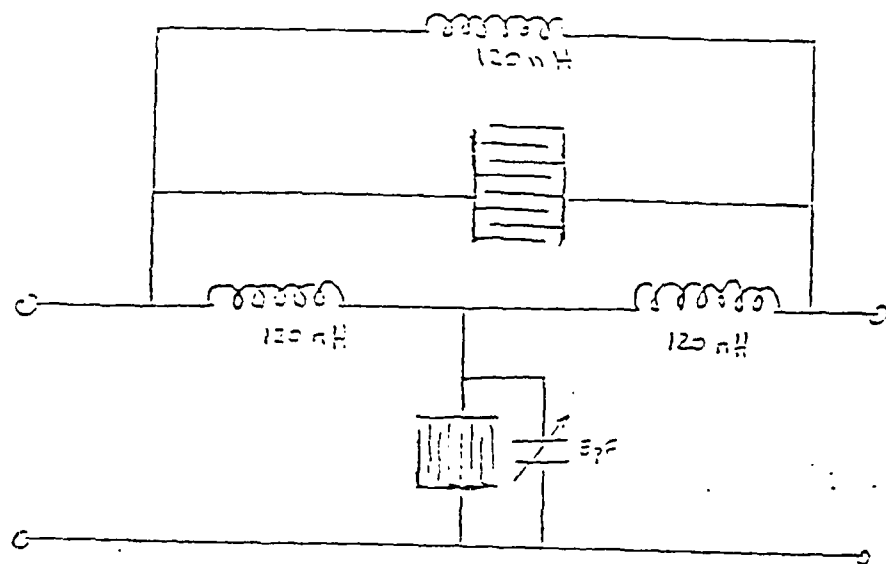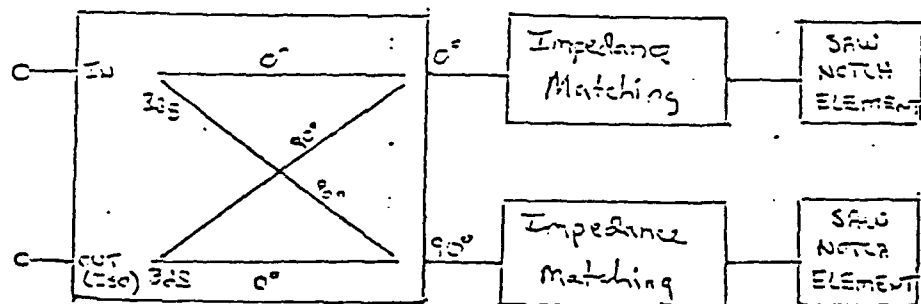
Figure 1.5 Quadrature Hybrid Notch
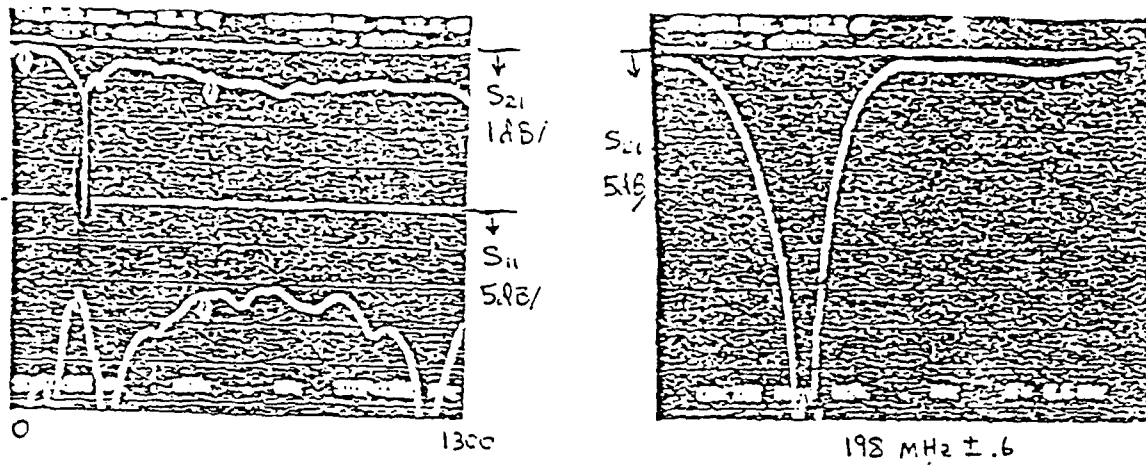
S_{21} /dB/

S_{11} 5.dB/

O 1300

S_{21} 5.dB/

198 MHz ±.6

Figure 1.6 Response of prototype bridged - T Filter

IN

MERRIMAC

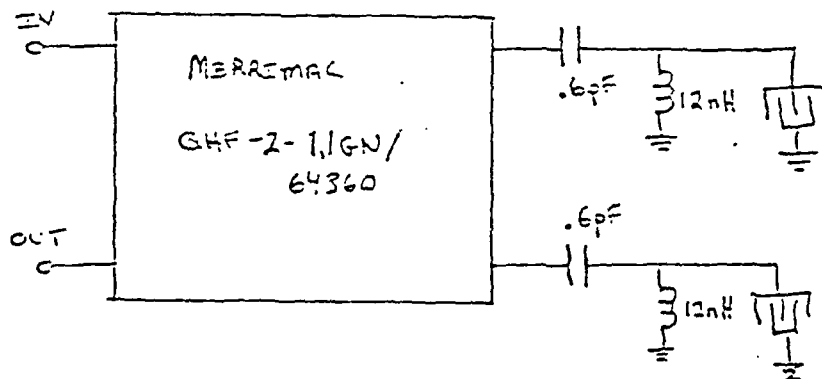GHF-2-1,IGN/ 64360

OUT

.6pF

12nH

.6pF

12nH

Figure 1.7 Prototype quadrature Hybrid Notch Filter

In the quadrature hybrid circuit, shown earlier in **Figure** 1.5, the SNE is matched to the characteristic impedance of the hybrid in the stopband, thus absorbing all input power. At all other frequencies, the SAWs are pure reactances, hence absorb no power. It is a property of quadrature hybrids that when both ports have identical reflections, all power is transmitted to the output ("isolated") terminal as shown.

The quadrature hybrid circuit has the ability to implement a wider stopband than the bridged-T. However, this is done at the expense of notch depth. Also, the passband width, loss, and ripple are primarily determined by the performance of the hybrid.

Figure 1.7 shows a quadrature hybrid notch filter which was developed for use as an output filter in a high power JTIDS transmitter. The filter was required to prevent spurious emissions into the IFF channel at 1030 MHz. **Figure** 1.8 shows the response of a prototype notch circuit. This filter used a quartz SNE to obtain a notch with a 20 dB stopband of 14 MHz and a 1 dB bandwidth of 60 MHz. The passband loss was 1.3 dB with a 1 dB passband from 300 MHz to 1600 MHz.

Table I compares some currently demonstrated capabilities of the bridged-T and quadrature hybrid circuits. Both circuits have their advantages and likely will find uses in practical applications. Other circuits have been investigated, however they did not accomplish the low insertion loss of the previously discussed circuits. The higher insertion loss is primarily due to the use of resistors in the signal path. **Figure** 1.9 shows some other circuits which have been investigated.
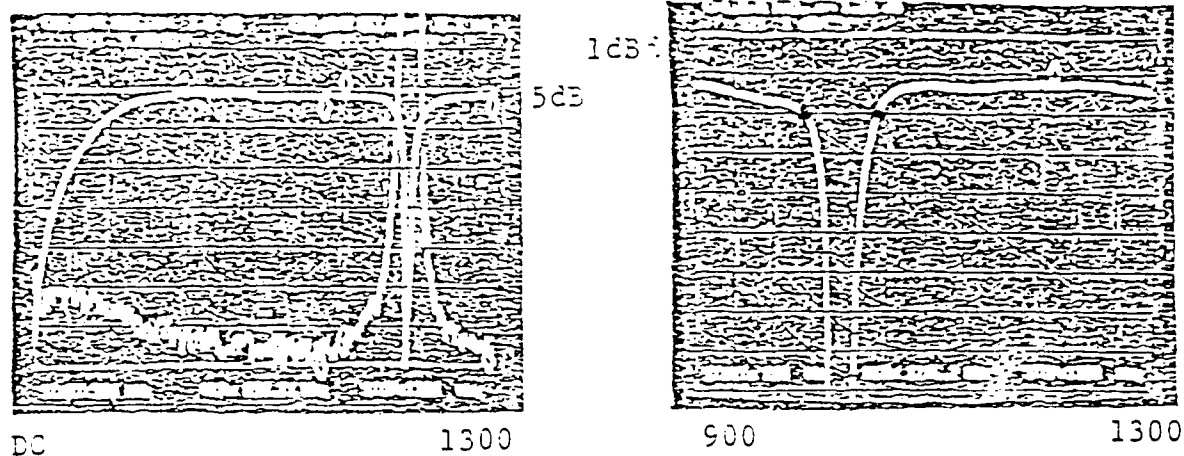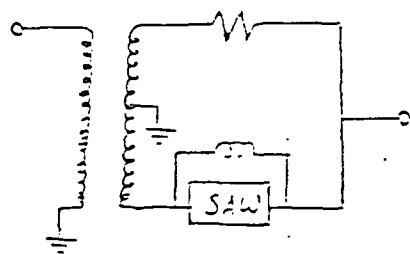
Figure 1.8 Response of prototype Quadrature Hybrid Notch Filter

Figure 2.9 Some other Notch Circuits

(a) Transformer Inverter
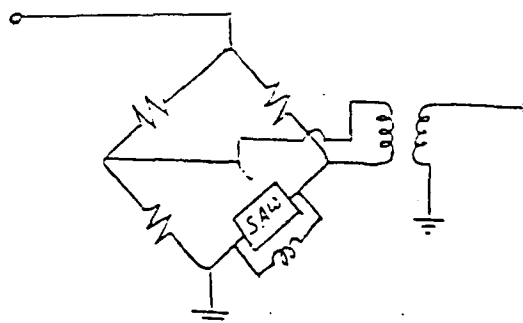
(b) Passive Wheatstone Bridge
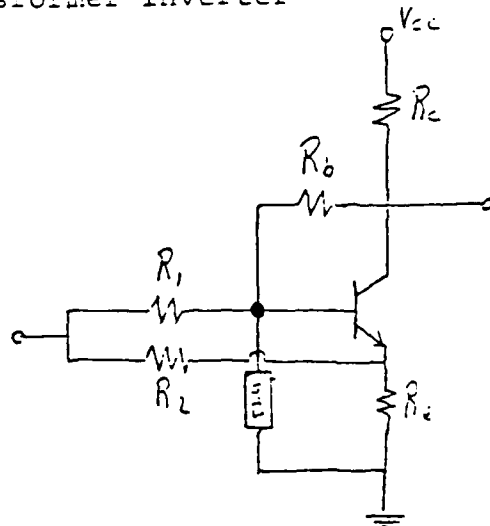
(c) Active Wheatstore Bridge

Currently Demenstrated Capabilitées of SAW
Notch Filters (per Section)

	Bridged - T	Quadrature Hybrid
Passband Bandwidth	> 10:1	Limited by Quadrature hybrid typically >2:1
Passband Loss	< 2 dB	< 2 dB
Stopband Rejection	45 dB	25 dB
Shape Factor (1dB : 40dB)	7:1	5:1
Maximum Stopband Width	0.05 %	1.5 %

Table 1

II. DEFINITION AND IMPLEMENTATION OF THE SAW NOTCH ELEMENT

Chapter 1 of this report outlined the previous research done on notch filters using SAW technology. The resulting filters are based on a two-terminal Surface Acoustic wave (SAW) device which is called the **SAW Notch Element (SNE)**. The SNE is a device in which the electrical properties of a SAW interdigital transducer are used to create predetermined admittance characteristics.

The admittance of a SNE is characterized by a band of frequencies exhibiting relatively constant conductance and susceptance. The conductance, which is caused by the conversion of electromagnetic power to acoustic waves, causes the electrical loss required to implement the stopband. The susceptance causes phase shifts which allows phase-balanced cancellation. This frequency band, over which the device admittance is relatively constant, is referred to as the **"flatband"** of the device. The lack of this "flatband" in previous SAW notch filter designs is responsible for the relatively poor shape factor. The remainder of this report will discuss the initial research on topics relevant to the analysis, design, and manufacture of SNE (SAW Notch Elements), as well as the circuits in which they are employed.

2.1 COMPARISON OF TRADITIONAL SAW NOTCH FILTERS TO THE SNE

SAW devices have become widely accepted for many signal processing applications in recent years. Typically, these monolithic devices convert the electrical signal into acoustic

waves which travel on the surface of a crystal before being detected as modified electrical signals. The acoustic waves are preferred for signal processing because of the size reduction allowed by their relatively short wavelengths (five orders of magnitude shorter than that of the electromagnetic waves).

Signal processing has been accomplished by the frequency selectivity of several different processes, including electro-mechanical transduction, mechanical reflections from a grating, mechanical resonances within a cavity, and coupling between acoustic beams by a multistrip-coupler. All of these signal processing techniques share one common feature, namely that the signal processing is accomplished by manipulating acoustic energy either during conversion, in transit, or in storage. Because of this, SAW devices are typically considered in terms of the signal transfer between two SAW transducers. Depending on the mechanical properties of the surrounding acoustic circuit, these filters are classified as either transversal filters or as resonant filters.

The SNE does not fit either classification. It is not a true transversal filter, since the signal in transit across the waveguide is not taken as the output, which is the common property of transversal filters. The device does not require resonances for its operation, as is shown by the FIR implementation, below.

The SNE is characterized by a single port admittance, $Y(\omega)$, corresponding to a device which dissipates power over a selective band of frequencies. Both the SNE and the one-port resonator may be considered subsets of a class of SAW devices which will be called admittance (or impedance) elements.

2.2 DEFINITION AND IMPLEMENTATION OF THE SAW NOTCH ELEMENT

The SNE admittance response is obtained by terminating the acoustic ports of a specially-designed SAW transducer, either with absorber or with a weakly-reflective grating. The transducer is designed in order to achieve a particular admittance function [5-7]. The desired features of the SNE are (a) high capacitive Q in the filter passband (low capacitive losses), (b) rapid transition from passband characteristics to stopband characteristics, (c) low capacitive Q in the filter stopband (high capacitive loss) and **(d) relatively constant admittance (both the real and imaginary parts) across the filter stopband.** Properties (a) - (c) are desirable in order to have good dynamic range or selectivity; however, the existence of a region having "relatively constant" admittance is crucial to the realization of practical SAW notch filters. The "constant" admittance requirement gives rise to the term "flatband" when discussing properties of the component, with the term "stopband" being reserved for discussion of the filter. (This term is also used in the description of coupled wave propagation to describe frequency bands for which $k(\omega)$ corresponds to a lossy wave.)

Figure 1.1 shows the input admittance of an ideal SNE. Figure 1.2 shows a physically realizable response. Since the device must be causal, the conductance and susceptance are related by the Hilbert transform [8]. The Hilbert transform places constraints on how rapidly the admittance may change from the previously discussed flatband properties to the passband properties, thus placing a lower bound on the transition bandwidth. The Hilbert Transform relationship is used to obtain the flattened susceptance around the resonant frequency. The existence of this "flatband", created by a

local minima between two conductance peaks and the associated inflection point in the susceptance, in an admittance element is the definitive characteristic of the SAW Notch Element (SNE). This feature allows the SNE to match the phase and amplitude of slowly-varying lumped elements over a larger fractional stopband width.

The SAW transducer appears to be a constant-valued capacitor at frequencies away from the SAW modes and bulk wave radiation. At frequencies which are near the resonances associated with the shear and longitudinal bulk waves, undesired responses are typically observed in the conductance. When used as a termination on a transmission line, an ideal transducer reflects all of the incident power except at the SAW response and at the frequencies of undesired bulk wave radiation. The broad bandwidth of the transducer's reflectivity is ideal for implementing the filter passband. The SNE should be used either as a capacitor in a lumped element filter, or within a one-port line termination in a multi-port transmission-line filter. The stopband and transition bands of the filter should use the lossy resonant characteristics of the transducer capacitance and its transition to lossless behavior.

2.3 IMPLEMENTATIONS OF THE SAW NOTCH ELEMENT

The SNE has been defined and discussed in terms of its ideal response; however, there has not been any discussion of the various potential techniques for implementing the device. There are several alternate techniques which may be used to obtain this conductance function. The flatband may be created by synthesizing two conductance peaks such that the separation between them is comparable to the bandwidth of the conductance peaks. The Hilbert Transform of this conductance waveform is capable of low susceptance variations over a finite bandwidth. Three fundamentally different approaches have been considered

to date. The desired response may be obtained (a) by the parallel connection of two transducers having single-peaked responses with the appropriate frequency difference, (b) by the FIR synthesis of a filter function which corresponds to the desired admittance function, and (c) by the use of internal mechanical reflections to implement a Single Phase Unidirectional Transducer (SPUDT), which naturally provides a very good approximation of the SNE response [9].

In method (b), the SNE admittance is synthesized by the same techniques which are used to shape the responses of SAW band-pass filters. The input conductance of a SAW transducer may be related to its transfer function by the Impulse Model of the SAW transducer [10]. This model discusses the relationship between the normalized radiated power of a FIR function and the associated normalized conductance. The SNE is obtained by designing a transducer with a transfer function which corresponds to the desired admittance of **Figure 1.2.**

This technique has been used for SNE's in the past; however, withdrawal weighting was used to implement most of these designs. Any method of implementing an FIR response by SAW filters will result in a conductance response which deviates from that predicted by the impulse model. Apodized (spatially weighted or overlap weighted) transducers have been analyzed by Malocha et al. [11]. The conductance responses are shown in the reference for several variations on simple overlap weighting. In general, there are spurious conductance peaks near the passband of the transversal filters. These same spurious responses may be present in apodized implementations of SNE's designed in this manner.

Withdrawal weighting, which is a narrow-band approximation to the desired FIR response, exhibits serious spurious conductance peaks, even over a wide frequency range [12]. These peaks result from spurious coupling to both the SAW and bulk waves away from resonance. The impulse model may be used to estimate these spurious conductance responses by examining

the transfer function of the transducer away from resonance.

The transducer length required is inversely proportional to the bandwidth of the conductance peaks on either side of the flatband. The two peaks are being implemented simultaneously, causing the device length to be increased. This method is preferred over method (a) in terms of parasitics and labor; however it is far from being the optimum method of implementing the SNE.

In method (c), the input conductance of an unweighted SPUDT (Single Phase Unidirectional Transducer) is used to approximate the desired SNE response [9]. The input conductance of the unweighted SPUDT naturally yields an admittance similar to the desired SNE response. The two peaks of the response are obtained by inserting a "valley" into the single-peaked conductance of a uniform conventional transducer. The "valley" is inserted by the addition of properly-phased internal reflections within the transducer. These reflections cause an "acoustic stopband", in which the reflections from the array of electrodes are in phase. This coupling between counter-propagating waves effects the input admittance by reducing the conductance near resonance. A "valley" is caused between the two resulting conductance peaks. The slope of the flatband susceptance is controlled by the magnitude of the internal re-flections in conjunction with the length of the device. The relationship between flatband slope, device length, and reflec-tion coefficient is rather complicated; however, unweighted uniform transducers typically require the product of the reflection coefficient and device length to be about 1.25.

The width of the "acoustic stopband" is proportional to the reflection coefficient. The device length is inversely propor-tional to the sum of the bandwidths of both of the peaks and the "valley". There is an indirect relationship between the device length and the reflectivity required to implement a flatband. This approach uses the shortest possible device length in order to implement the SNE, thus the device will have the lowest static capacitance of the proposed methods. On the

other hand, very narrow flatbands typically require very thin metal in order to achieve the low reflectivities which are associated with these long devices. The resulting film thickness will likely prove to be an ultimate limitation for extremely narrow notch filters at high frequencies. This problem may be overcome to a certain degree by the use of reflector "thinning", in which, for example, every N^{th} reflector is used. Reflector thinning may have undesired side effects since the reflectors are being opperated at a harmonic, allowing the grating to scatter the SAW into bulk waves.

2.4 THE NATURAL SPUDT (NSPUDT)

There are many alternative methods which can be used to create a SPUDT; however the Natural SPUDT, which uses two $\lambda/4$ electrodes of alternate polarity per wavelength and single-level fabrication, has been preferred [13]. The $\lambda/4$ electrodes exhibit the highest conductance-to-capacitance ratio, giving the lowest flatband Q, of any transducer geometry. The Natural SPUDT (NSPUDT) requires the use of custom substrate orientations and propagation directions; however the technology uses the same materials and processes as the manufacture of SAW resonators and filters. One NSPUDT orientation of quartz, which has been made public, employs the common ST wafer with propagation along an axis rotated +/- 25° from the crystalline X axis [14].

III. RESULTS OF PHASE I WORK: CURRENT PROJECT STATUS

3.1 STATUS OF TECHNICAL OBJECTIVES OF PHASE I

Phase I of this contract consisted of several technical objectives. These included (1) the definition of a comprehensive model for SNE analysis, (2) development of an experimental technique that may be used to determine some of the model parameters, (3) determination of the performance trade-off's based on the model, and (4) plan the Phase II research required in order to improve the modeling and design techniques required for SAW notch filters to be readily available.

In addition to the work performed on each of these objectives, additional research effort was directed toward immediate problems in the development of production SNE's. This add-itional work, which was to be performed under Phase II, was at least partially customer funded and includes (a) the software for effective permittivity calculations which was written for the principle consultant, (b) literature search for papers on thin film properties of metals, (c) the modeling of 'series-weighted' transducers, and (d) the software for the four-port model of a single-mode device "increment" with associated network cascading routines.

OBJECTIVE 1: THE MODEL OF A SAW NOTCH ELEMENT (SNE)

A comprehensive model of the SNE is defined in the first monthly report. This model includes provisions for multiple SAW modes, bulk wave radiation, and buss-bar effects. The SNE model defines several new terms which are applied to various

stages of the analysis. One of the principle goals of the model is to incorporate the various properties of the substrate and metalization, such as finite buss-bar impedances, finite bond-wire admittances, and spurious acoustic modes into the Coupling-of-Modes (COM) analysis of the SAW transducer [15]. Another goal of the model is to describe a systematic approach for the addition of structural and material information as the analysis proceeds from the ideal and abstract levels to the non-ideal and physical levels. For example, the ideal incremental transducer results when one combines data for several electrodes from the sample file with the corresponding structural (geometrical) data describing the physical dimensions of the device and material data describing the substrate and metal film.

The most abstract level of the model is the **"sample file"**, which describes the electrical and mechanical properties of each transducer electrode in normalized units. The final level of the model is the **"device"**, which consists of the two-port S-parameters of the packaged SNE placed in series with the signal path and suspended over the ground plane.

Intermediate levels of the model are defined, with each new level adding a new, non-ideal term to the analysis. The ideal **"increment"** of a transducer describes the properties of a group of samples which are connected by ideal buss-bars, adding material factors and acoustic interactions to the **"sample file"**. A "segment" includes the effect of finite buss-bar impedance and describes the properties of a portion of the device between bond-wire locations. The **"transducer"** includes the effects of finite bond-wire admittance. **Figure** 3.1 shows the **"segment"**, consisting of six "increments" and their asso-- ciated buss bar parasitics. The bond wire admittances are included, so that the figure describes a portion of the device at the "transducer" level.

The **"element"** level, the next level of the model, has two components, the **"COM Element"** and the **"Effective Permittivity Element"**. The "COM Element" adds the effects of end reflec-

tions and finite chip size, or absorber, to the coupled mode analysis used above. The other component of the "element" describes bulk wave radiation directly from an electrostatic analysis of the "sample file" and a material function known as the effective surface dielectric constant [16]. The addition of package parasitics to the COM and bulk "elements" yields the desired "device" parameters. This model includes all of the effects of which we are aware, except finite width, either explicitly or implicitly. Some of the COM variables, implicitly contained in the model, may not be included in the current software. An excerpt from the first monthly report is included in Appendix A.
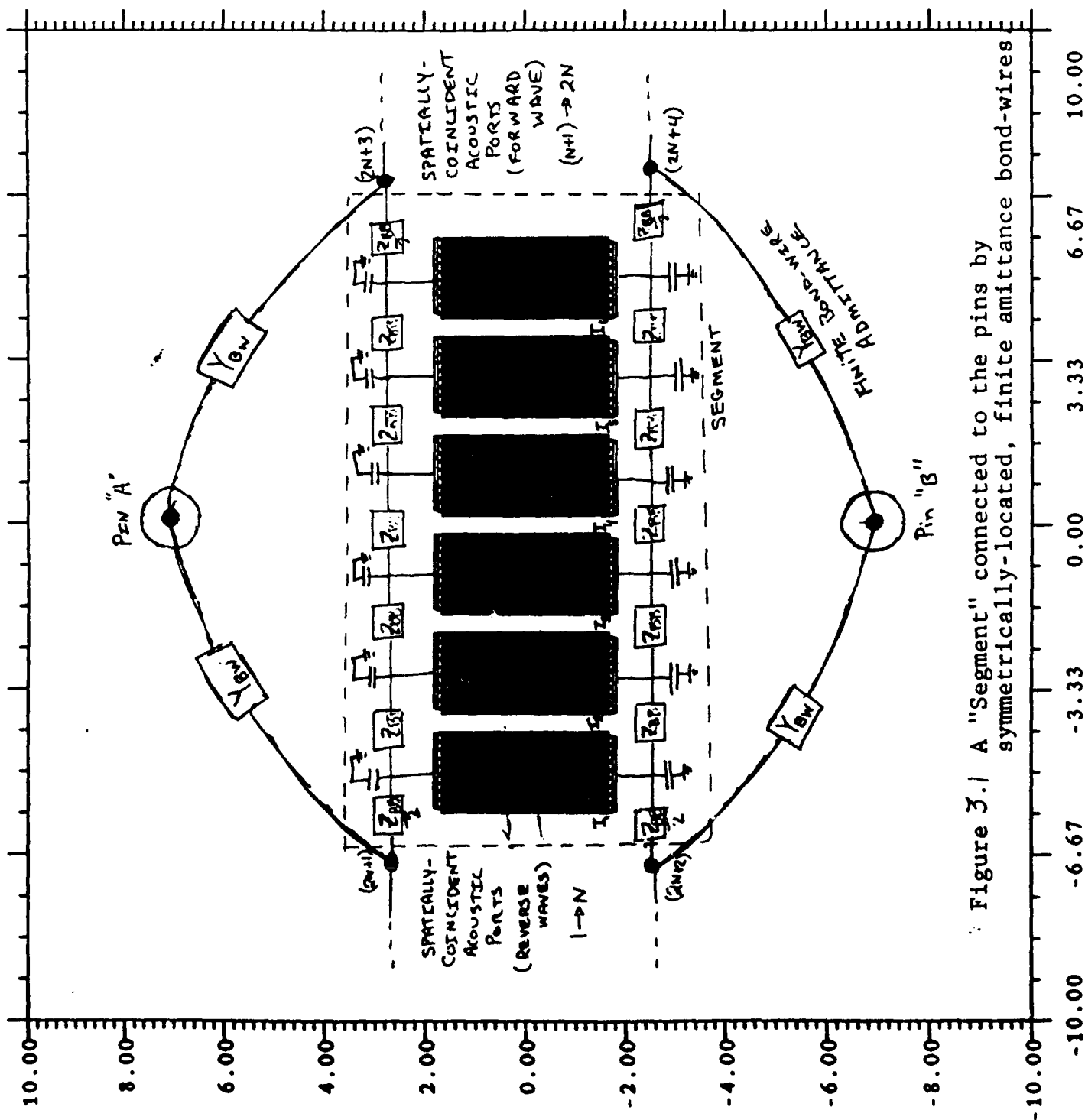
Figure 3.1 A "Segment" connected to the pins by
symmetrically-located, finite amittance bond-wires

OBJECTIVE 2: EXPERIMENTAL DETERMINATION OF MODEL PARAMETERS

Experimental Procedure for the
Determination of Model Parameters

Some of the effects which degrade the response of a SAW Notch Element (SNE) must be characterized experimentally. These are the effects caused by diffraction, buss-bar parasitics, bulk wave generation and improper beam steering compensation. Tests have been designed to isolate these effects.

Surface Acoustic Wave (SAW) transducers often generate surface acoustic waves with a power flow which is not in the direction of the main axis of the waveguide structure (Figure 3.2.a). The angle between the direction of power flow of the SAW and the main axis of the transducer is refered to as the "power flow angle." It is possible to compensate for the power flow angle by angling the electrodes of the transducer as shown in Figure 3.2.b. To determine the effect of not having the fingers angled the correct amount, the test mask has been divided into quadrants. Each quadrant has a different power flow angle compensation as depicted in Figure 3.3. The electrodes of the test devices will be angled by 0, 2, 4 or 6 degrees depending on which quadrant they correspond to. Each quadrant has a group of parts which is identical to the parts of the other three quadrants except that the electrodes are angled by a different amount.

Within each of the quadrants, there are devices with transduction lengths of 1000λ and 2000λ. Half of the 1000λ devices have beamwidths of 5λ, the remainder have 20λ beamwidths. Half of the 2000λ devices have 5λ beamwidths, the remainder have 40λ beamwidths. Different beamwidths correspond to different transverse mode behavior. Transverse modes are the
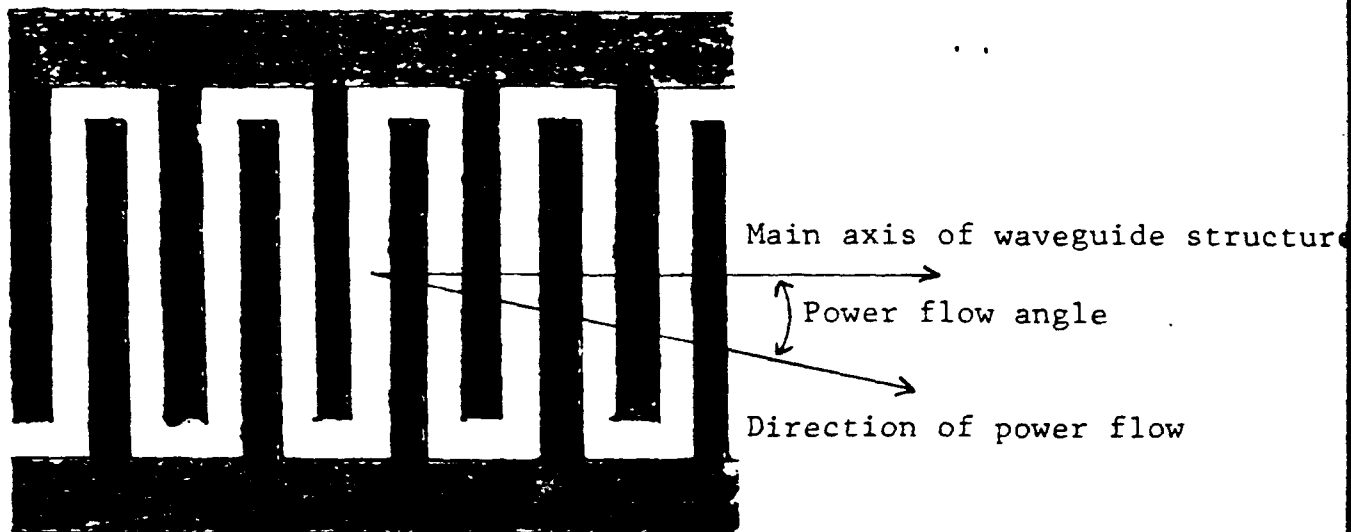
Main axis of waveguide structure

Power flow angle

Direction of power flow

Figure 3.2.a Power flow angle.

Direction of power
flow is compensation
to be along main axis
of waveguide struc-
ture

Figure 3.2b Power flow angle compensation.

Devices in this region have 0° power flow angle compensation.

Devices in this region have 2° power flow angle conpensation.

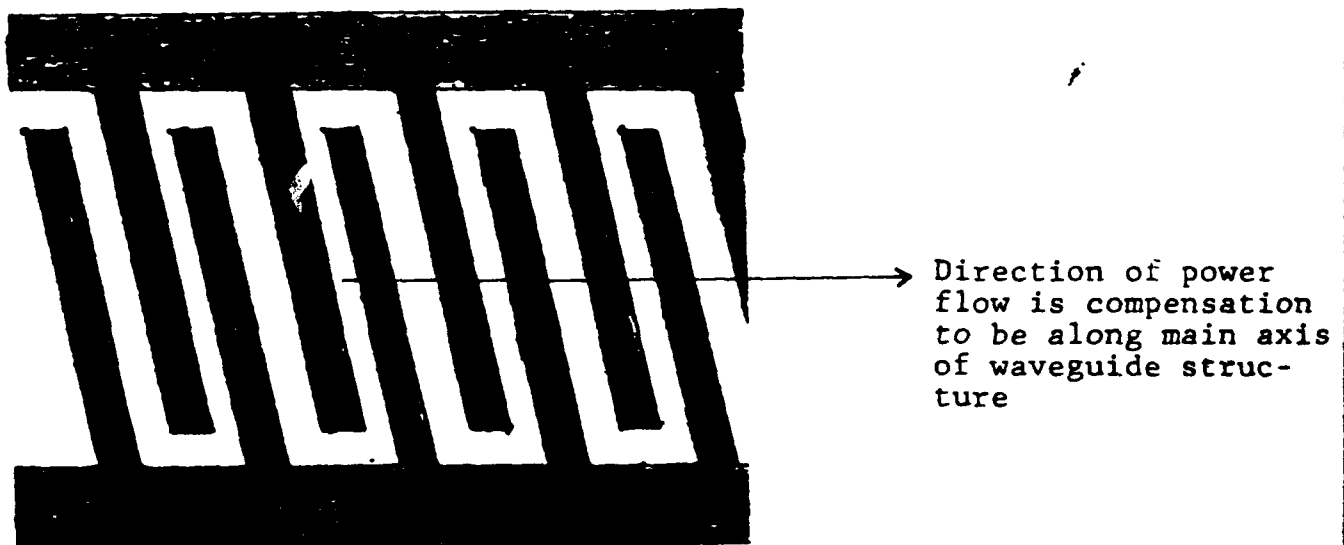Devices in this region have 4° power flow angle compensation.

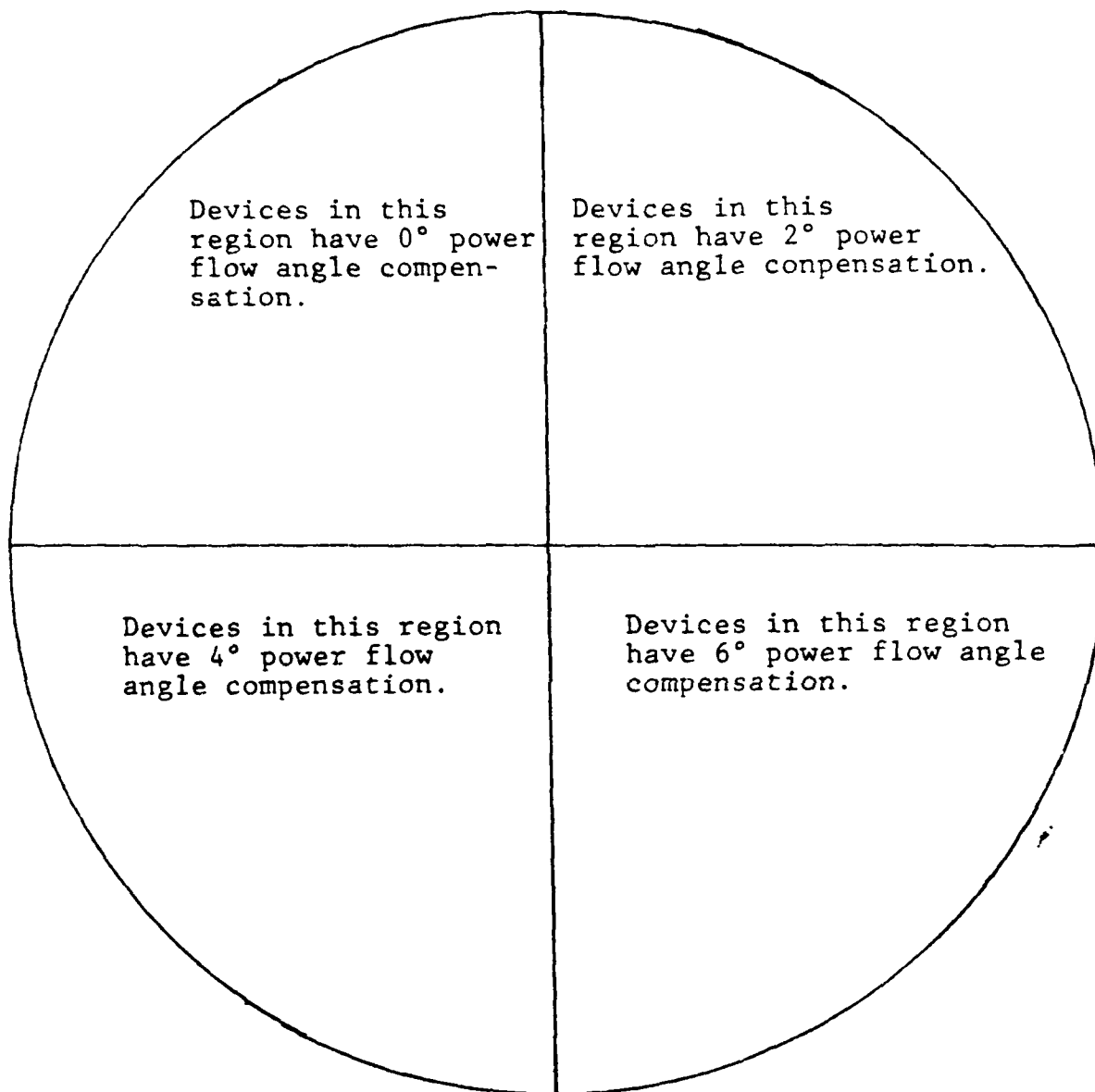Devices in this region have 6° power flow angle compensation.

Figure J.J Mask layout for power flow compensation.

primary effect of diffraction within the SNEs.

All of the structures discussed above are repeated three times with three different buss-bar widths. The widths are $50\mu m$, $100\mu m$ and $200\mu m$. The variation in buss-bar width will change the buss-bar resistance and inductance. The values of the buss-bar resistance and inductance can be measured and their effects will be obvious since the devices will be identical in every other way.

Bulk modes are generated by SAW transducers. Bulk modes can be characterized by carefully measuring the response of the SNE around the frequencies of the bulk modes. The effective permitivity program discussed in the first monthly report will be used to determine the frequencies at which the bulk modes will be generated.

Data Reduction Procedure

The data reduction procedure extracts the values of several material parameters by fitting the theoretical Coupling-of-Modes (COM) model of a SAW transducer to the measured data. The COM model currently predicts the S-parameters of a transducer in terms of the geometrical parameters, (length, width, and number of electrodes per wavelength), the material properties (dielectric constant, C_0, leakage conductance, G_0, piezoelectric coupling, k^2, acoustic reflectivity, $|\kappa| < \phi_\kappa$, and the propagation loss, γ), and a mixed parameter, F_0. The magnitude and phase of reflectivity, dielectric constant, and piezoelectric coupling are the values of most interest. These variables also have the most pronounced effect on the admittance function. The remaining variables have been included in order to obtain a better fit to these parameters. The center frequency could, in principle, be used to obtain the SAW velocity; however, resonator measurements are more accurate. The attenuation (propagation loss) has very little effect on the admittance for aluminum. This parameter was added to the parameter list in

order to extract the properties of silver and gold films. The leakage conductance of the substrate was added in an attempt to extract data from lithium niobate and lithium tantalate measurements.

The procedure may be outlined as follows. A device is measured on an Automated Network Analyzer (ANA) with the value of S_{11} stored in the computer. The program then reads in this data and converts it to the array "exp_y". The value "eps" is calculated as the RMS value of "exp_y". This value is used to normalize the error later in the procedure.

The user is then asked to guess values for the various parameters. These parameters are used to calculate the array "the_y". A squared error is evaluated as

$$\text{sqr\_err} = [\sum_{i=1}^{\text{npts}} |(\text{exp\_Y}_i - \text{the\_Y}_i)|^2]/\text{npts}$$

which is the square of the RMS error. This function is evaluated once for the trial values and once for each parameter being changed by one increment (as the others are held constant). If the changes in the error function were divided by the corresponding incremental changes, a gradient would be defined. This was not done since some variables have much more pronounced effects on the admittance than others and it may be desireable to lower some of the sensitivities.

Once all of the incremental differences are evaluated, the trial values are modified. If the parameters are represented by X_i, the increments by Δ_i, and the changes in the error function by δ_i, then the values of X_i are changed by

$$X'_i = X_i - \Delta_i(\delta_i/\delta_{max}).$$

This technique is similar to the well known steepest descent technique. The routine has been tested for transducer length of 100 to 200 wavelengths with beamwidths of 100 wavelengths. The agreement in these cases was excellent for aluminum on quartz.

For the test structure which has been built, $|\kappa| = 0$ at F_o and $k^2_{eff} = 0$ at $2F_o$, so that a simpler (fewer variables) version of the algorithm may be implemented. In this case, only

C_o, G_o, γ, k^2, and F_o need be used. On the other hand, the long devices will probably not yield accurate extracted data unless buss-bar parasitics are included.

OBJECTIVE 3: DESIGN CAPABILITIES AND TRADEOFF'S

The study of design capabilities has proven very worthwhile. The Principle Consultant has expressed the insertion loss of the SAW filter in terms of the normalized SNE conductance. The conductance is scaled to unit value at the center frequency. The expression assumes that the SNE susceptance is due to a constant-valued capacitance, and is not strictly valid in the transition band. However, in the passband of the circuit, the expression readily predicts the insertion loss incurred by undesired conductance. The expression has been obtained for both the Bridged-T and Quadrature Hybrid circuits. These design curves have isolated a major limitation on the shape factor of current SNE-based notch filters.

The SNE is a terminated SAW transducer, with an input conductance caused by the radiation of acoustic waves. Hartmann's impulse model is often used to relate a transducer's acoustic sidelobe levels to the associated spurious conductance levels [10]. Based on this simplified model, one observes that if no acoustic power is radiated, there is no electrical conductance. This observation is only strictly valid when the acoustic energy is equally distributed across the width of the device. In spatially weighted (electrode overlap weighted) transducers, it is possible for the net acoustic radiation across the width of the device to be zero, while there may be significant radiation in any small section, or track, of the device. This has led to a significant degradation in the shape factor of all existing SAW notch filters.

In addition, the modeling of the "notch depth vs. width" trade-off may be possible. For the Bridged-T circuit, one must determine the critical value of Q_f, the flatband Q of the SNE,
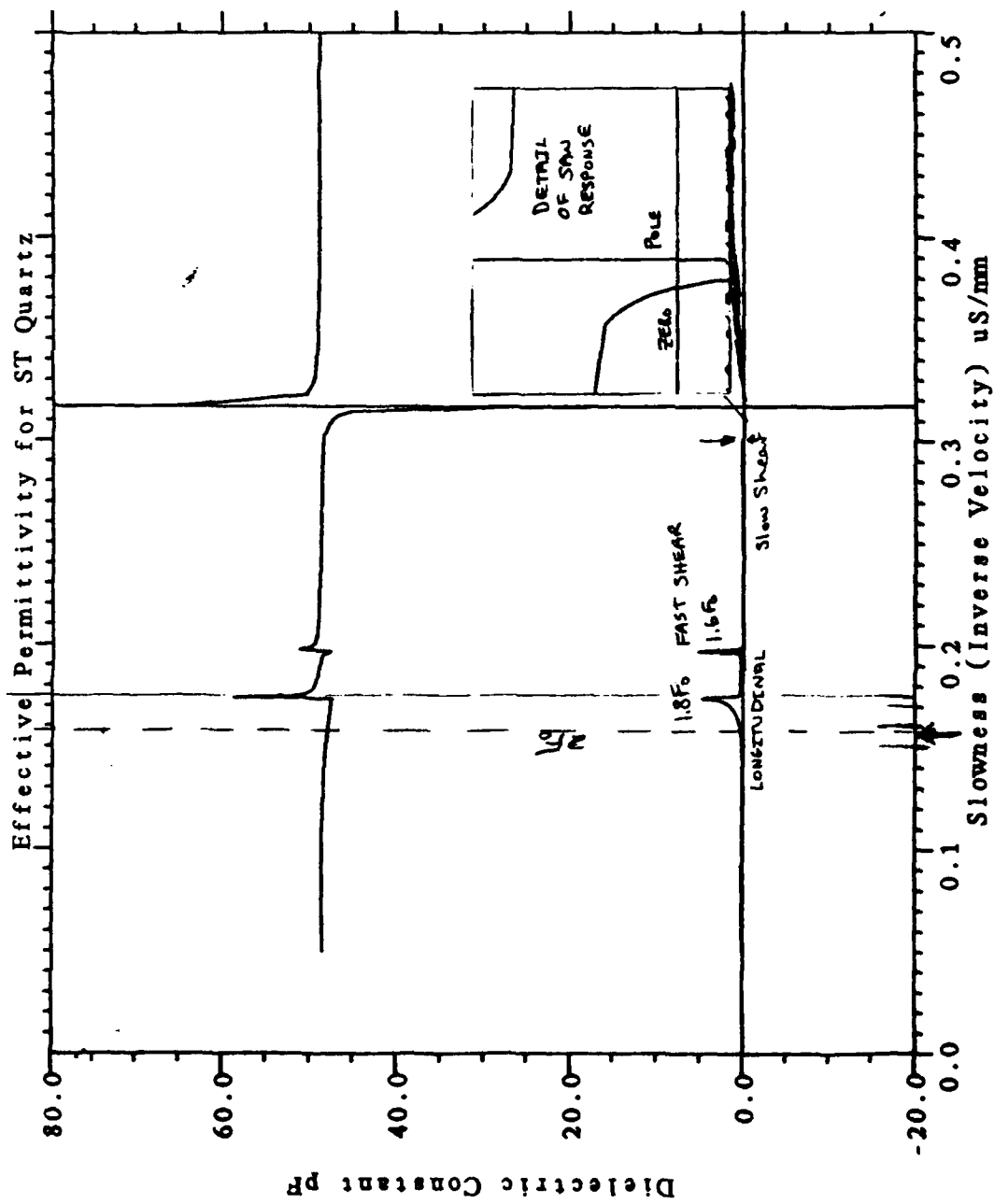
Figure 34 Effective Permittivity of ST Quartz

as a function of the voltage transfer ratio. Given Q_f, one must determine the widest stopband which may be implemented on a given substrate with the desired SNE structure.

3.2 RESEARCH PERFORMED DURING PHASE I IN ADDITION TO (3.1)

Software Development - Effective Permittivity

During Phase I, other work was performed which was intended as Phase II work. During the first month, a computer program was written to evaluate the "effective permittivity" of a SAW substrate [16]. This program was written with partial support from the Principle Consultant's contract with ET&DL, #DAAL01-87-C-0749. The software is required in order to model the contribution of bulk wave radiation in the SNE.

The "effective permittivity" of a material is defined for a given propagation direction in the surface plane and relates the spatial harmonics of charge and voltage. On a piezoelectric substate, the function has a pole at the metalized SAW velocity and a zero at the free surface SAW velocity. Additionally, the function will have a pole-zero pair off the real axis for a leaky wave (Pseudo-SAW). The leaky wave sometimes occurs within the bulk spectrum as a surface wave which radiates energy into the bulk and decays as it propogates. Finally, the function contains all of the information on bulk wave radiation as loss term. Figure 3.4 shows an example of the "effective permittivity" function for ST quartz.

As the program exists, an infinite beamwidth is assumed, therefore there are no transverse modes. With significant modifications to the software, a finite beamwidth can be assumed. This will account for transverse modes in the device. The transverse modes are a fundamental description of diffraction effects in a guided structure, while free surface diffraction is typically analyzed as a beam-spreading phenomena.

Continued Implementation of the SNE Model

As we mentioned earlier, the smallest sub-division of the SAW transducer model is the "increment." An increment is a portion of a transducer which has ideal buss-bars. The "increment" has two electrical ports (one for each buss-bar), and 2N acoustic ports, where N is the number of surface modes. The four port S- parameters of the increment have been derived in terms of the current three port model. Figure 3.5.a shows the three port transducer as a four port device with one of the electrical ports shorted. Figure 3.5.b illustrates some of the effects of symmetry on the transducer.

In addition to the derivation above, general cascading routines have been developed. These include (a) parallel connecting the ports of a two-port to form a one-port, (b) placement of a two-port between two of the ports on a four-port network, and (c) other "glue" routines required to analyze series-weighting. Finally, the series-weighting analysis was written. This analysis is outlined below, along with some initial results.

Improved Device Weighting

The Principal Consultant presented a plot of passband insertion loss (at a given frequency) in terms of the SNE conductance (at that frequency) relative to the center frequency loss. The relationship is repeated in Figure 3.6. Since most specifications discuss a 1dB bandwidth in conjunction with 1dB pp ripple, this level has been indicated on the figure. Taking the worst case, the Bridged-T circuit, the maximum conductance out-of-band may be specified as 4.5%, which is lower than the conductance of the first sidelobe for a uniform transducer. Considering the acceptable level of group delay variation, which is a more stringent factor, limits the rapid conductance variations in the sidelobes of the transducer to about 2% of the center
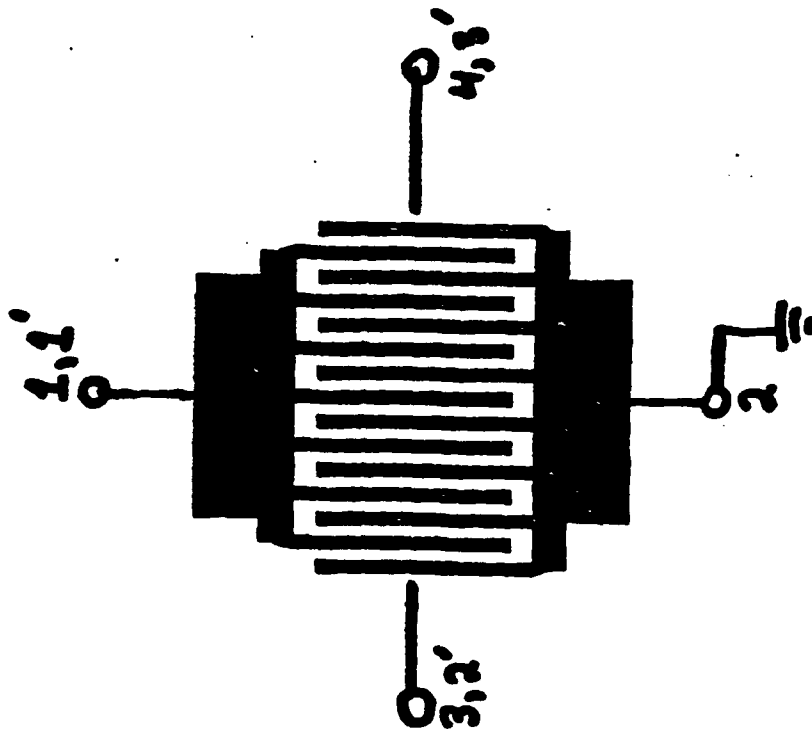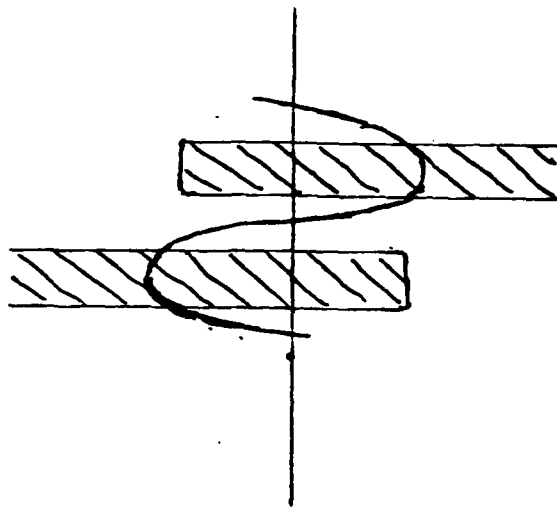
INTERCHANGING PORTS 1 AND 2 WILL
CAUSE A SIGN CHANGE IN TRANSDUCTION.

$$S_{2J} = -S_{1J}$$
$$S_{I2} = -S_{I1}$$

FIGURE 3.5.6 EFFECT OF SYMMETRY ON
PORT 2 TRANSDUCTION.

FIGURE 3.5.a THREE PORT SAW TRANSDUCER
(1',2',3',) REPRESENTED AS
A FOUR PORT (1,2,3,4)

Pass Band Loss vs Gout/Gin

+ = Bridged-T;   x = Quad Hybrid
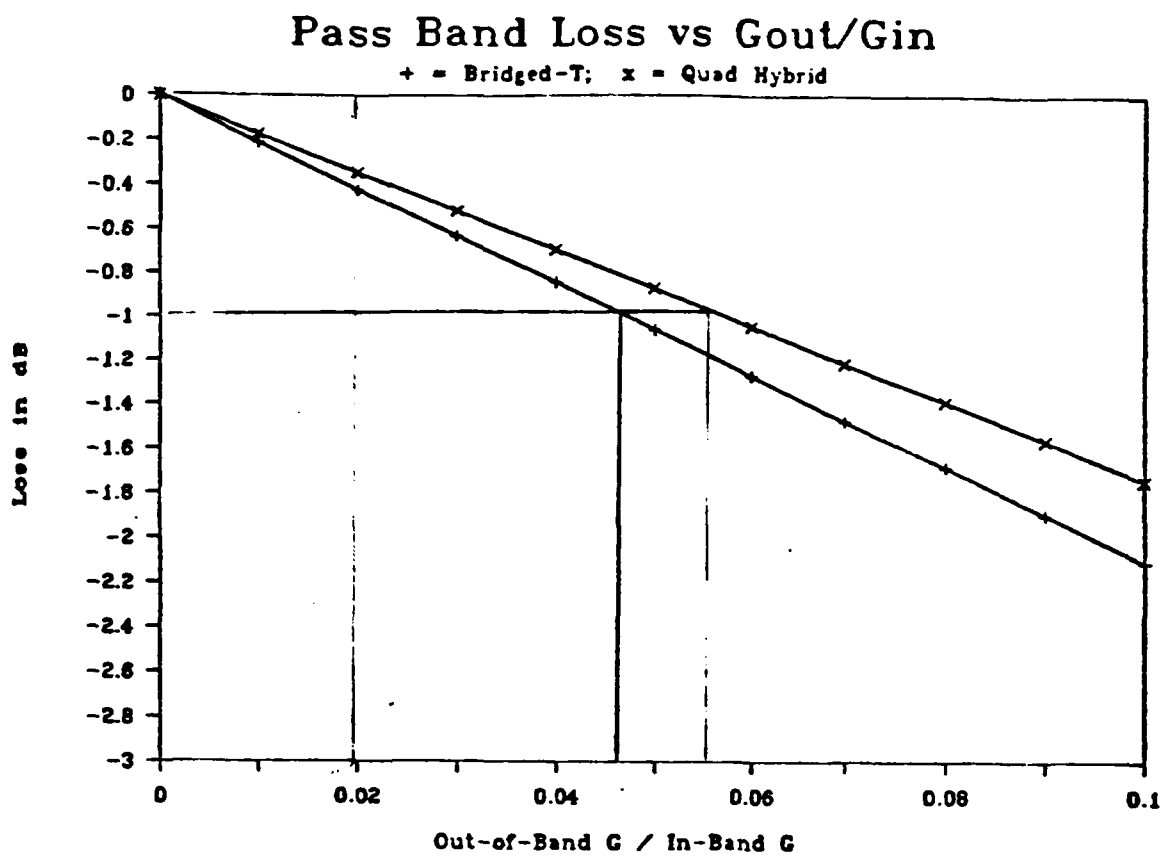
Out-of-Band G / In-Band G

FIGURE 3.6 RELATIONSHIP BETWEEN RELATIVE CONDUCTANCE
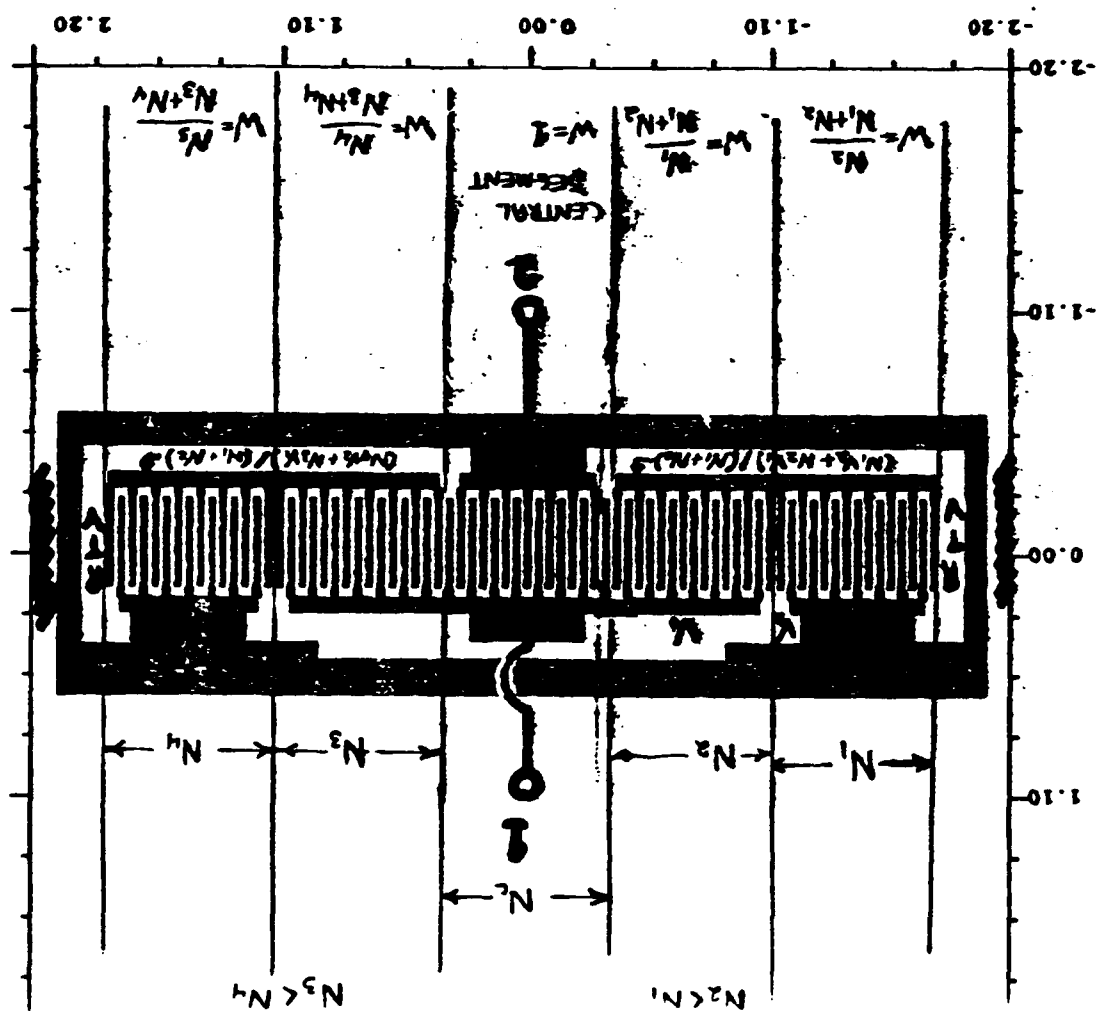AND INSERTION LOSS.

frequency value.

The passband ripple must be reduced without sacrificing shape factor. An improved weighting technique, called series weighting, has been proposed and modeled. Figure 3.7 shows the general structure of a series-weighted transducer. The series electrical connections within the transducer cause voltage division, which is used to implement the weighting. This voltage division has two effects, it causes the series-connected portions of the transducer to have a relative transduction strength (the weighting); but also, it lowers the device admittance due to the properties of admittances in series. Although there will be a significant dependence on the specific weighting function; this technique will lower the device admittance by about 40% relative to a uniform transducer.
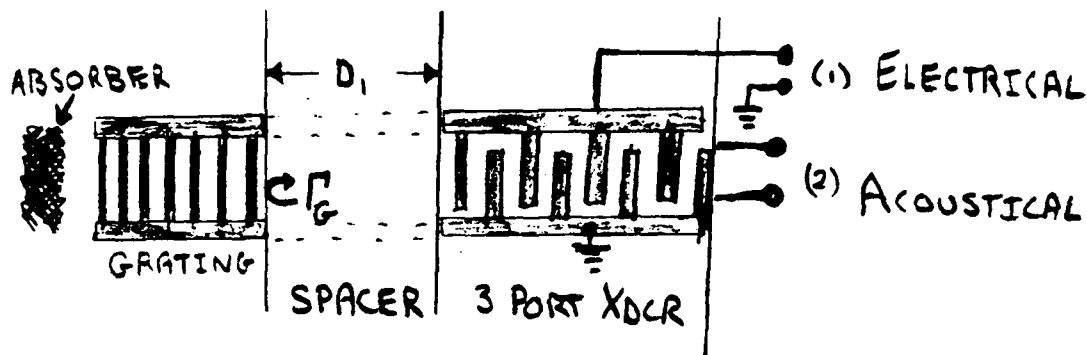
This device has been modeled, assuming ideal buss-bars, no bulk wave generation, and a single SAW mode. The analysis evaluates the S-parameters for the left and right side series-connected "transducer increment" pairs. This evaluation begins with either a (one-port) termination, or a one-port grating cascaded with a transmission line spacer. The resulting one-port network terminates the outer acoustic port of a three-port "transducer increment", as shown in Figure 3.8.a.

The resulting two-port, representing interactions between electrical energy and inner-port acoustic energy, is placed between port 1 and the outer acoustic port of a four-port "transducer increment". This implements a series electrical connection of the "increments" with current flow from electrical port 2 of the inner "increment" to ground. The acoustic ports are cascaded sequentially, just as they appear on the substrate. The outer acoustic ports have been terminated, being port 3 on the left and port 4 on the right. The remaining acoustic port completes the resulting two-port. Figure 3.8.b illustrates the structure of the left side network using block diagrams. The right side network follows from symmetry.
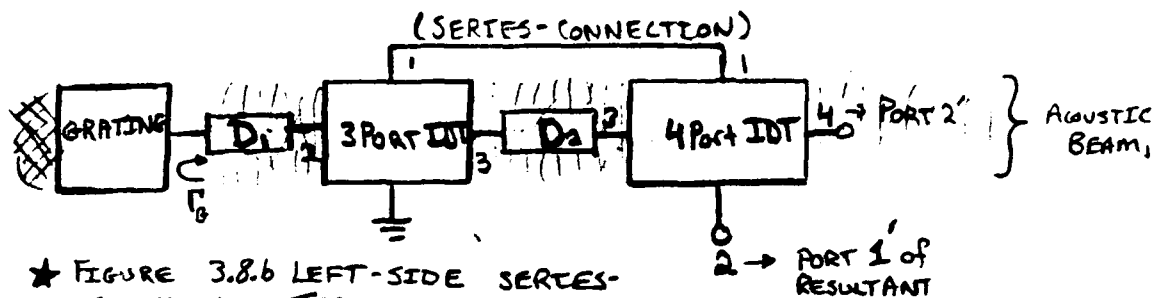
Next, the central "increment" is evaluated, and the electrical port (1) is switched with ground. The left side network is

ABSORBER

D_1

(1) ELECTRICAL

(2) ACOUSTICAL

Γ_G

GRATING

SPACER | 3 PORT XDCR

★ FIGURE 3.8.a TERMINATION OF "OUTER" ACOUSTIC PORT
BY A SPACER AND GRATING

(SERIES-CONNECTION)

GRATING — D_1 — 3 PORT IDT — D_2 — 4 Port IDT — 4' → PORT 2' } ACOUSTIC BEAM,

Γ_G

2 → PORT 1' of RESULTANT

★ FIGURE 3.8.b LEFT-SIDE SERIES-
CONNECTED TRANSDUCERS

LEFT

(1)
CENTRAL: REV.
POLARITY 3 PORT
IDT
(-1)

2' | 2

3 → 3" } ACOUSTIC BEAM

{ACOUS (2)}

ABSORBER

1' → 2"

1"

Internal Parallel Connection

{ELEC (1)}
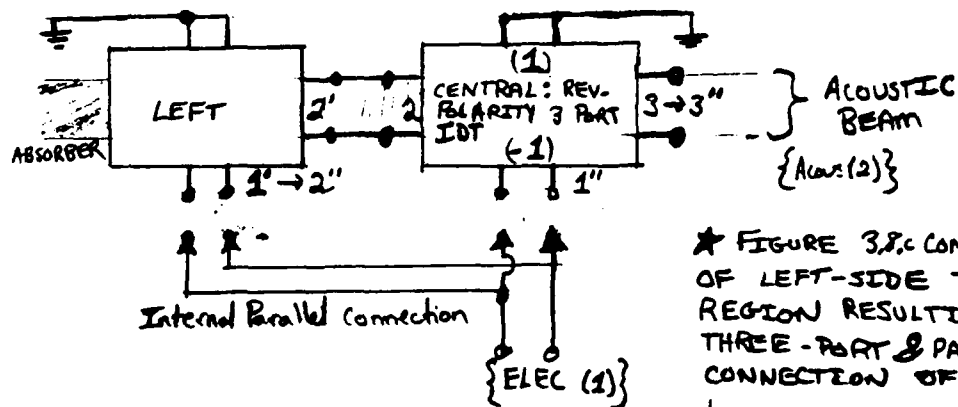
★ FIGURE 3.8.c CONNECTION
OF LEFT-SIDE TO CENTRAL
REGION RESULTING IN A
THREE-PORT & PARALLEL-
CONNECTION OF TRANSDUCERS.

★ FIGURE 3.8.d PURELY ELECTRICAL
TWO-PORT. PARALLEL CONNECTION
(DASHED) COMPLETES THE SNE.

ABSORBER | LEFT / CENTRAL | D_3 | RIGHT | ABSORBER

ABSORBER

ACOUSTIC
BEAM (WAVEGUIDE)

(1) (2)
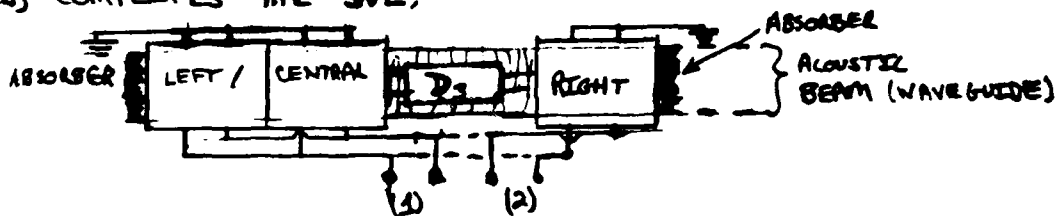
acoustically cascaded onto the central network, resulting in a network with two electrical ports. Figure 3.8.c shows the connection and the resulting three-port. The two electrical ports are parallel connected, leaving a two-port. The right side network is then attached to the left / central network by the acoustic ports, leaving a purely electrical two-port network, as is shown in Figure 3.8.d. These electrical ports are parallel connected, resulting in the one-port model of the series-weighted SNE.

Figure 3.9 compares the transducer admittances of two alternate series-weightings with an equivalent-bandwidth uniform weighting. The ripples are suppressed with no significant impact on the shape factor. There appears to be some undesired skewing of the conductance function for the asymmetric structure.

Thin Metal Film Studies

During the third month, an initial literature search was done to understand the effects of very thin metallic films. Most SAW devices employ metal films with thicknesses ranging from about 600 Angstroms to about 10000 Angstroms. Due to some of the fundamental properties of SNE's, the metal thickness is significantly thinner than that used by other devices at the same frequency. For example, at 200 MHz, a typical transversal filter would use between 1000 and 2000 Angstroms of aluminum and a typical resonator might use 5000 Angstroms. In contrast, the CATV SNE's discussed below use between 500 and 650 Angstroms.

One of the most significant papers which was located discussed the measurement of the mass density of aluminum films with thicknesses between 250 and 2000 Angstroms. A significant variation is seen below about 650 Angstroms [17]. The study of thin film properties of aluminum is planned for this phase of the research. Silver and gold may also be investigated for comparison, although both metals are commonly attributed with high acoustic losses.
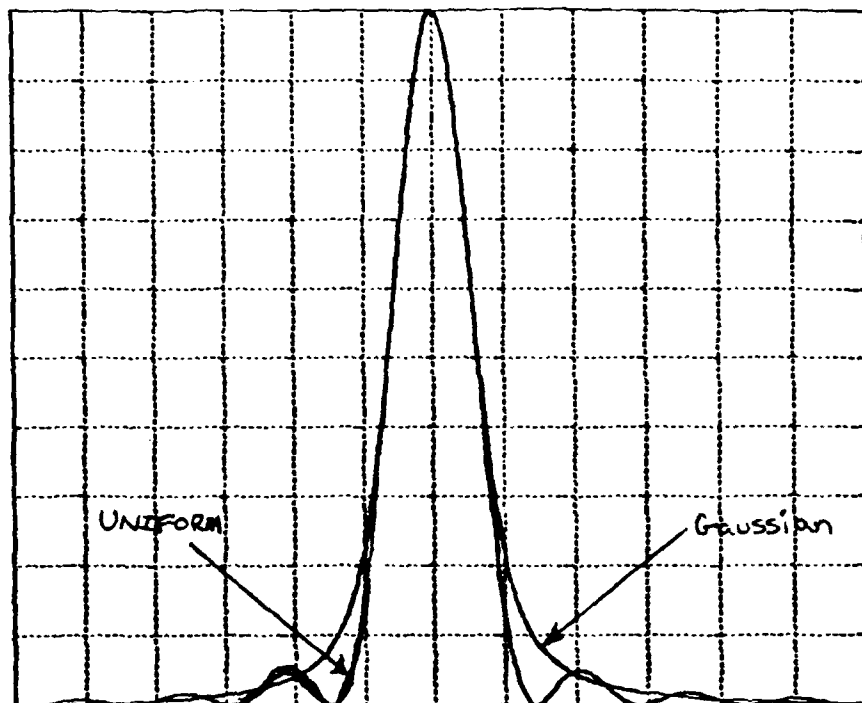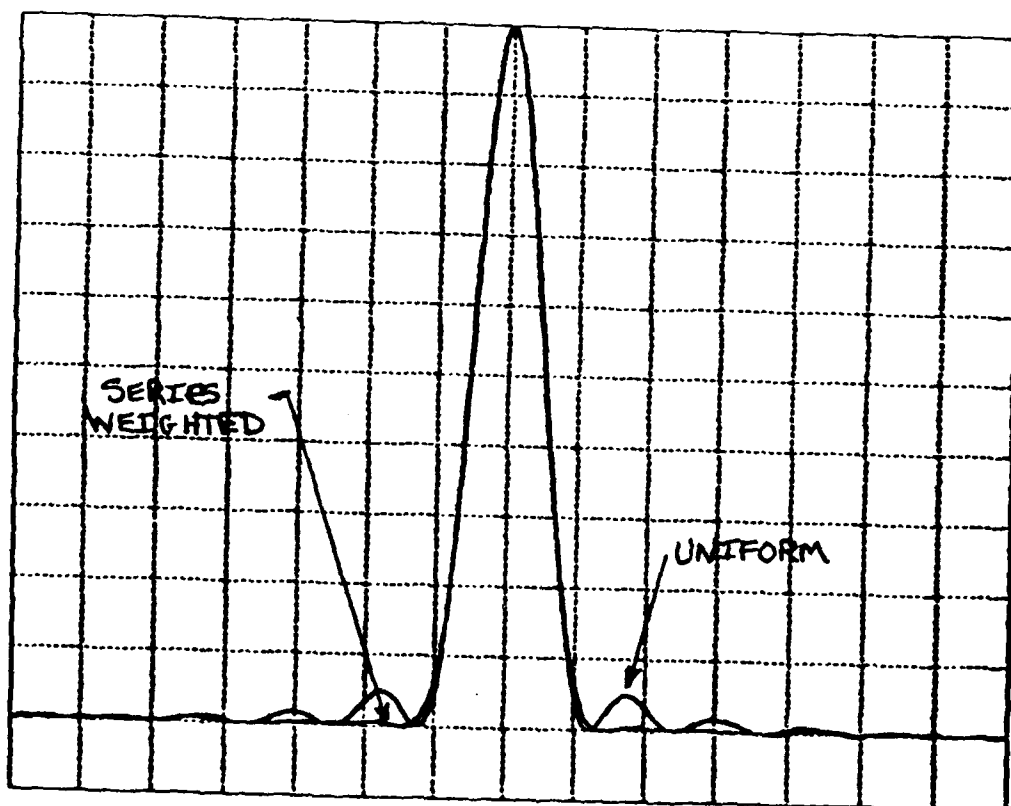
FIGURE 3.9.a GAUSSIAN AND UNIFORM

FIGURE 3.9.b UNWEIGHTED AND SERIES WEIGHTING

Phase Tuning

Another topic studied during the third month was the possibility of trimming the flatband by using resistively terminated reflective gratings within the SNE. The ability to trim the slope of the SNE's flatband susceptance was demonstrated. This dimension of design freedom will be further investigated during Phase II.

3.3 ESTIMATE OF TECHNICAL FEASIBILITY

The results under Phase I have been very encouraging. Objectives (2) and (3) have not been completed; however the results to date are extremely positive and have added new insight into the design of SNE's. Several unexpected problems with the manufacture of a high-volume SNE were encountered. Many significant advances have been made in the design, manufacture, and testing of SAW Notch Elements; as well as the circuits in which they are used.

As results were obtained under these objectives, new ideas and solutions relevant to the contract were realized. The effort was preferentially steered toward current design and manufacturing problems, availibity and manufacturability being the ultimate goals of the SBIR program.

3.4 SUGGESTIONS FOR FURTHER RESEARCH

The Phase I program has provided a foundation for significant technology advances in SAW notch filters. RFM will submit a proposal for Phase II work which will include advances in several areas as outlined below.

A. Completion of Comprehensive SNE Model

Under the Phase I program, a comprehensive SNE model was

defined. However, this modeling task has only been started under the Phase I effort and significant experimental and theoretical work remains to be completed. For example, some of the key parameters in this new model include the parasitic resistance, inductance and capacitance associated with the device packaging. Many of these parameters will need to be determined by means of extensive experimental measurements. Also, the parasitic loss due to bulk wave radiation is an important element in the new model. Extensive theoretical calculations of the effective permitivity of various substrates will be required to properly model this loss mechanism.

B. Optimum SNE Design Synthesis

At the present time, all SNE devices are implemented by synthesizing a "concave upward" input conductance for a SAW transducer. This produces the impedance characteristic that has real and imaginary parts which are approximately constant over a desired stopband range. It appears that one might be able to define modifications to this simple "concave upward" shape which would result in even more constant impedance over the desired frequency range. Developing methods for both defining such shapes and then synthesizing them with a SAW device will be a primary purpose of a Phase II program.
This optimization is similar to the optimization of SAW impulse responses for achieving low sidelobes in SAW bandpass filters. However, this problem is distinctly different in that the real and imaginary part of the input admittance are related by a Hilbert Transform whereas the frequency response of a SAW filter and its impulse response are related by a Fourier Transform. Thus, the methods used for optimizing SAW filter impulse responses will not apply directly to this optimization problem.

C. Improved SAW Notch Circuits

As described earlier, RFM has already achieved good SAW notch filter performance using both the bridged-T circuit and the quadrature hybrid circuit. However, it is possible that other circuits are feasible which will have better performance or other desirable characteristics. For example, it would be very desirable to eliminate all inductors from the notch circuits. This is probably feasible by using a stripline quadrature hybrid coupler but this would lead to rather large structures in the 225-400 MHz band.

Another desirable feature would be an agile SAW notch filter. At the present time, there is no clearly defined method for implementing an agile notch. If a method for creating an agile notch was discovered, the utility of SAW notch filters would be greatly enhanced.

D. Optimum Combinations of Notch Circuit and SNE

At the present time, the design method for SAW notch filters consists of first designing a SNE with a reasonably constant impedance across the desired filter stopband and then trying to define a circuit which will deliver the desired notch filter performance using this particular SNE. However, it is intuitively obvious that one might achieve greatly improved notch filter performance if one could design both the circuit and the SNE simultaneously. One could probably compensate for undesired circuit characteristics by changing the design of the SAW Notch Element and vice versa. For example, one might find that the best SNE design is one in which the impedance is not exactly constant across the desired stop band. The current design procedure would not reveal such possibilities. In a Phase II program, such optimum combinations will be investigated.

E. Solution to Practical SAW Notch Filter Problems

In the limited work to date on SAW notch filters, RFM has

discovered several practical problems which if solved could significantly enhance the usefulness of this new technology. Several of these problems will be discussed here, but only some of these will likely be part of a Phase II program.

One of the topics under the Phase I program will be investigation of the performance limitations of the SAW notch filter technology. If these limitations were reduced to a series of design curves then one could easily decide if a given application can be satisfied with SAW notch filters.

As discussed earlier, the SAW notch filters should be capable of handling large amounts of power in the passband region. Accurately determining the factors which limit the power handling will allow further increases in power handling and should open new applications for this technology.

In many cases, the ultimate performance of SAW notch filters will actually be determined by parasitics of the SNE package. Investigation of improved packaging methods should result in further improvements in notch filter performance.

To date, the best SNE devices have been implemented using NSPUDT structures. However, SNE devices can also be implemented using conventional SAW and resonator SAW transducers.

Also, there are several other types of SPUDT structures other than NSPUDTs and it is very likely that some of these will be superior to NSPUDTs in certain applications. For example, the Electrode Width Controlled SPUDT (EWC/SPUDT) being developed by Hartmann Research, Inc. can be used on ordinary SAW crystal orientations thus avoiding the beamsteering problems of most NSPUDT devices.

APPENDIX A

A COMPREHENSIVE SNE MODEL

Extensive discussions were held with Clinton S. Hartmann concerning the nature of a SNE (SAW Notch Element) model. Parasitic elements of the model were discussed and classified as either distributed or lumped. Examples of distributed parasitics are electrode and buss-bar impedances. Examples of lumped parasitics are bond-wire impedance and pin parasitics.

The device parasitics to be considered in a SNE model are: electrode resistance, propagation loss, buss-bar resistance, buss-bar inductance, capacitance to the case, transducer-radiated bulk waves, higher-order SAW modes, surface modes other than the SAW (leaky wave, etc.), incoherent bulk wave radiation under the buss-bars, bond-wire inductance, bond-wire resistance, pin-to-case capacitance, pin inductance, and pin resistance.

Electrode resistance, propagation loss, and other surface modes may all be treated within the coupling-of-modes equations. The buss-bar parasitics (R,L,C) are distributed, and could be included in the coupling-of-modes equations. This would cause significant complications to the COM equations. Instead, these parasitics are lumped and periodically placed along the resulting ideal buss-bars. Surface modes other than the SAW may be treated as additional coupled modes, along with the higher-order SAW modes. All bulk waves will be treated by the previously discussed "effective permittivity" theory. The pin parasitics are lumped at the i/o terminals.

A.1 DEFINITION OF THE VARIOUS LEVELS IN SNE MODEL

The model has been divided into several levels of complexity, based on which parasitics are included at that level of the model. Lower levels of the model describe only a portion of the entire device and are separated by lumped parasitics or discrete elements, such as bond-wires. The lower levels of the model are the most abstract and idealized. For instance, the lowest level consists of a **sample file**, which defines the electrode overlaps, material data, and geometrical data of the structure. The exact nature of this data has not been determined; however, the current software at RFM will be used as a starting point. This level of the model contains no parasitics.

The next level of the model is the **increment**, which is an idealized portion of the transducer having perfect buss-bars. The increment has two electrical ports, one at each buss-bar, and two mechanical ports for each acoustic mode (SAW, transverse modes, leaky wave, etc.). Increments are extracted from the sample file such that (1) they contain no bond-wire locations, and (2) the lumped buss-bar impedance has a small effect on the static capacitance of the increment. Figure A.1 depicts an increment with buss-bar parasitics lumped around it. The increment contains electrode resistance, buss-bar capacitance to the case, propagation loss, and other surface modes. An increment may contain any other distributed parasitic which may be added to the coupled-mode equations. Note that some distributed parasitics, if added to the equations, could make the analytic solutions, required for efficient modelling, impossible to obtain. This is precisely the reason that the buss-bar parasitics are lumped between increments. Each increment has a closed-form solution to the COM equations.

Each bond-wire location will define a **segment** boundary. For N surface modes, the segment is a (2N+4) port device. Four of these ports are electrical and represent the ends of each buss-bar. The remaining 2N ports are the forward and reverse acoustic ports for each acoustic mode. A segment contains
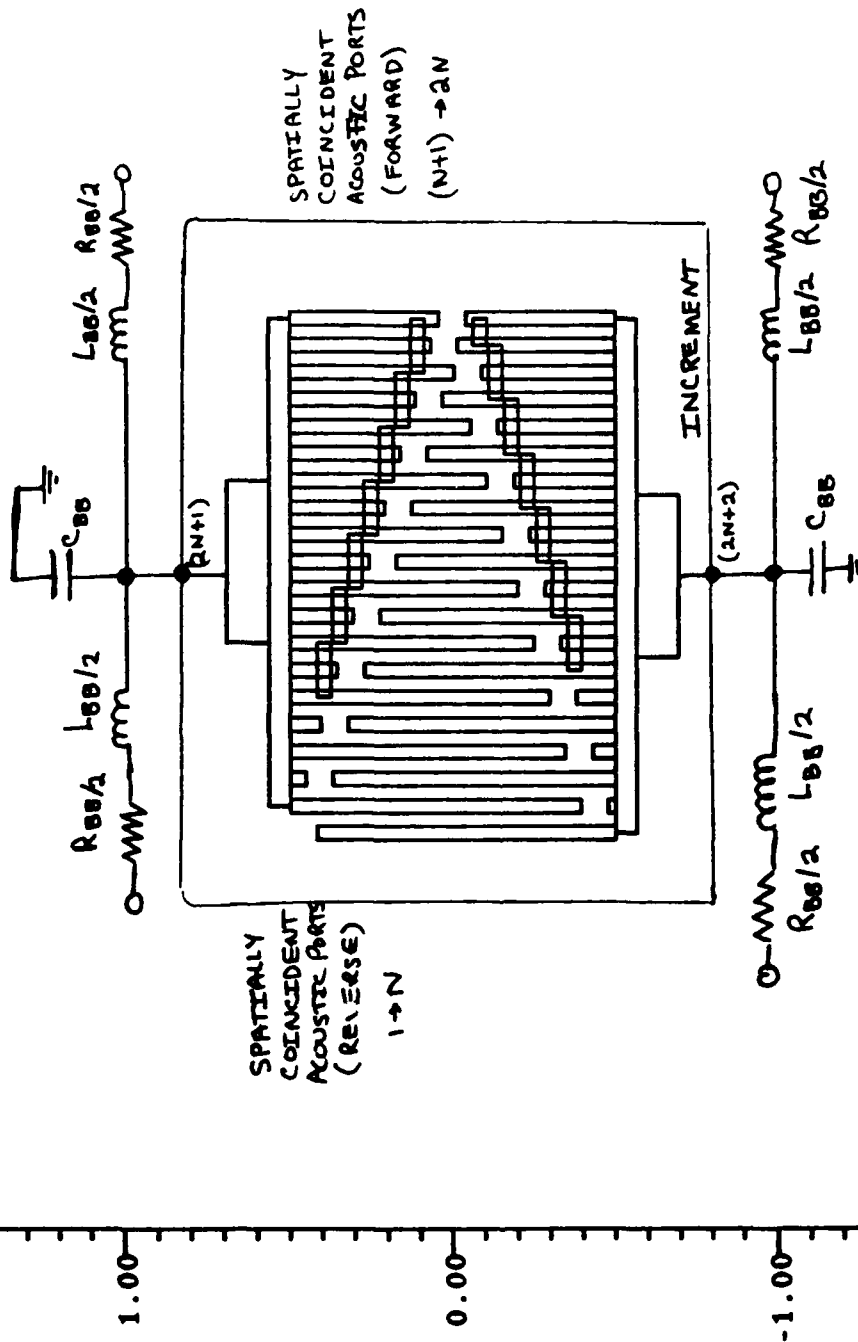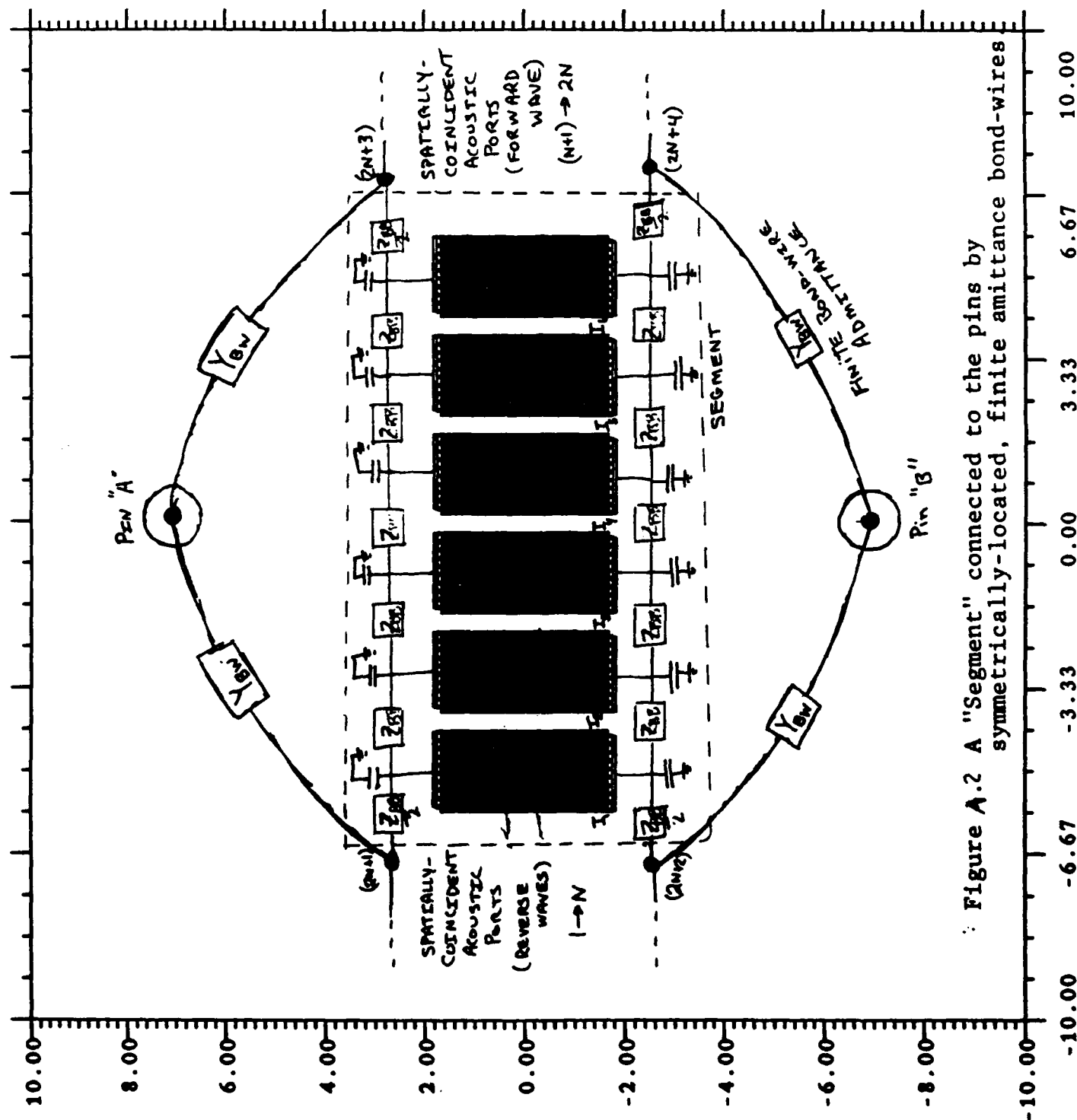
Figure A.1 An Idealized "Increment" with its associated
Parasitics.

lumped buss-bar parasitics and ideal transducer increments. An increment is determined and then evaluated by the COM analysis. The electrical ports are then connected to the centers of the buss-bar impedances. The increment with parasitics has the form of a segment; however, a segment will typically consist of several increments, with associated parasitics, in cascade. A segment is depicted in Figure A.2, with bond-wires connecting it to the pins. Note that symmetric bond locations are assumed. The analysis does not require this, since each bond-wire has a finite admittance (non-zero impedance) associated with it. This allows a bond-wire to be effectively removed by setting its admittance to zero.

The next sub-structure to be defined is the **transducer**, which will be a (2N+6) port structure. Ports 1 through N are the N reverse acoustic ports, ports N+1 through 2N are the N forward acoustic ports. Ports (2N+1) and (2N+2) are the reverse buss-bar terminations, while ports (2N+3) and (2N+4) are the forward buss-bar terminations. Ports (2N+5) and (2N+6) are the electrical ports at the top of the package pins. Figure A.3 depicts a transducer in its Scattering Matrix form.

Up to this point, no specific limitations have been imposed on the model, and it may be equally used for isolated transducers (SNE's) or embedded transducers in transmission-type filters. Since the sample file, as currently exists in the software, allows cavities to be defined, both 1-port resonators and transducer-based SNE's may be evaluated. Allowing the model to be used for SNE's having stopbands ranging from the material Q limit (narrow limit) to the matching network Q limit (broad limit).

The next step is to terminate the acoustic ports (model the acoustic absorber) and the buss-bar electrical ports (typically with open circuits). The resulting 2-port is the **COM element** which includes all of the properties of the SNE except the pin parasitics and the bulk wave radiation. Bulk wave radiation occurs in two forms, coherently transduced waves which are launched by the transducer as a broadside antenna, and

Figure A.2 A "Segment" connected to the pins by symmetrically-located, finite amittance bond-wires
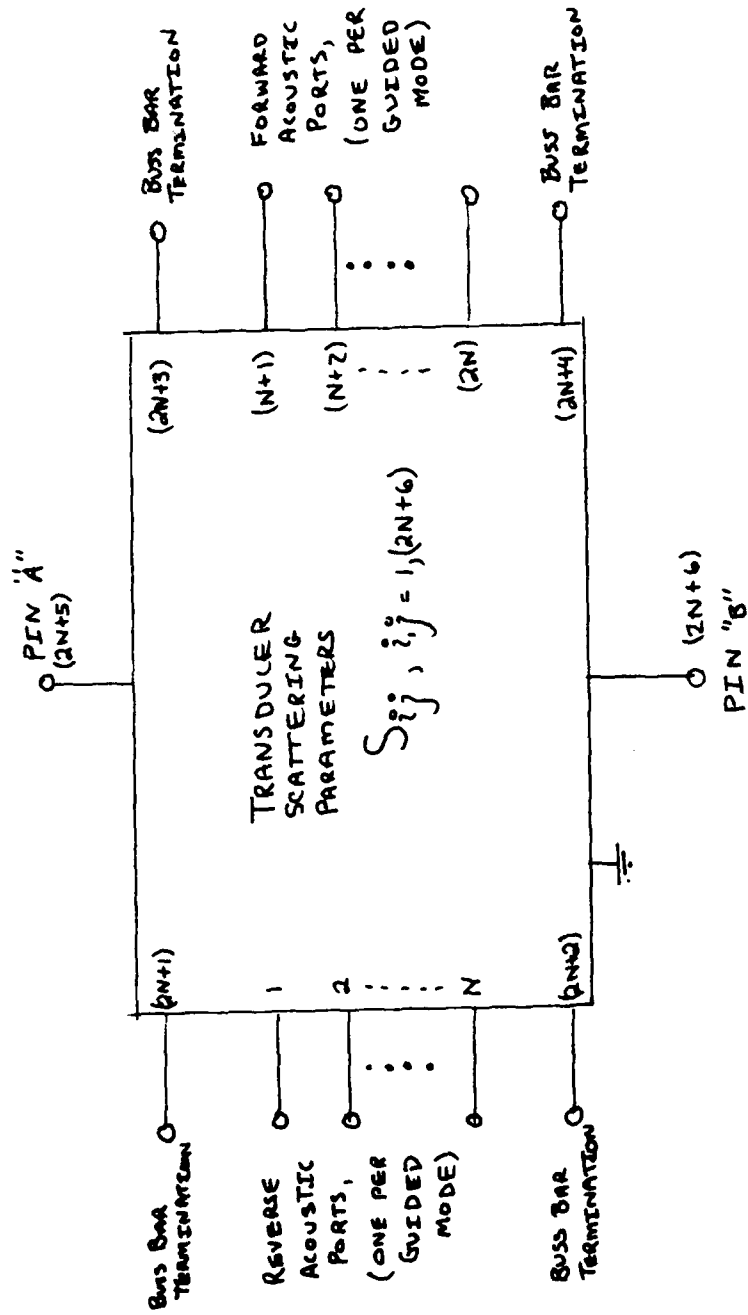
:: Figure A.3 Multiport representation of the SAW Notch Element model at the "Transducer" Level.

incoherent radiation which occurs in the bulk of the crystal. The incoherent radiation of bulk waves corresponds to high overtones of the bulk resonances with poor backside polish. Rather than a series of equally spaced bulk wave overtones, succesive overtones have lower and lower Q, eventually smearing into a continuum of radiation. A cross-section of a transducer is shown in Figure A.4a with approximate E-field lines. Figure A.4b shows a transducer launching three coherent bulk modes as a broadside antenna.

In order to evaluate the increment boundaries, a rough electrostatic analysis will need to be performed. From this, an estimate of the actual electrode voltages may be obtained. These voltages may be used (or the ideal constant voltages may be used) to evaluate the bulk wave radiated energy. This 2 port Pi network is the effective **permitivity element**. The shunt arms of the pi represent radiation of incoherent bulk waves in the parallel plate capacitor between the buss-bar and case ground. Each of these assumes zero overlap. The series arm of the Pi network consists of two parallel-connected components. One corresponds to coherent (transducer) bulk wave radiation. The other is a negative-real component which accounts for the reduction in the parallel plate capacitor radiation (shunt arms) due to the transducer overlap. Figure A.5 shows the device, including the COM element, the effective permittivity element, and the pin parasitics. This is the comprehensive model of a SNE.
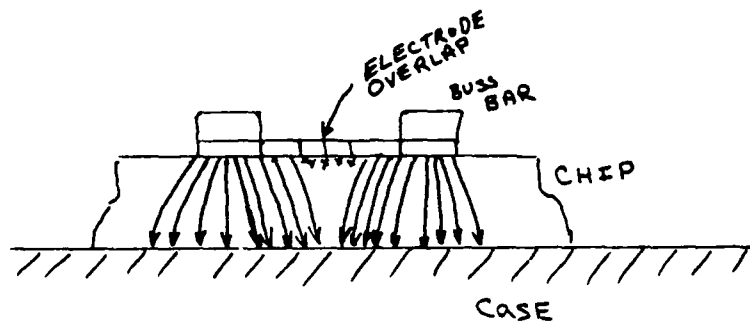
A.4:a. E-Fields under the buss-bars and electrodes in a SNE.
Note the reduction in field intensity under the active
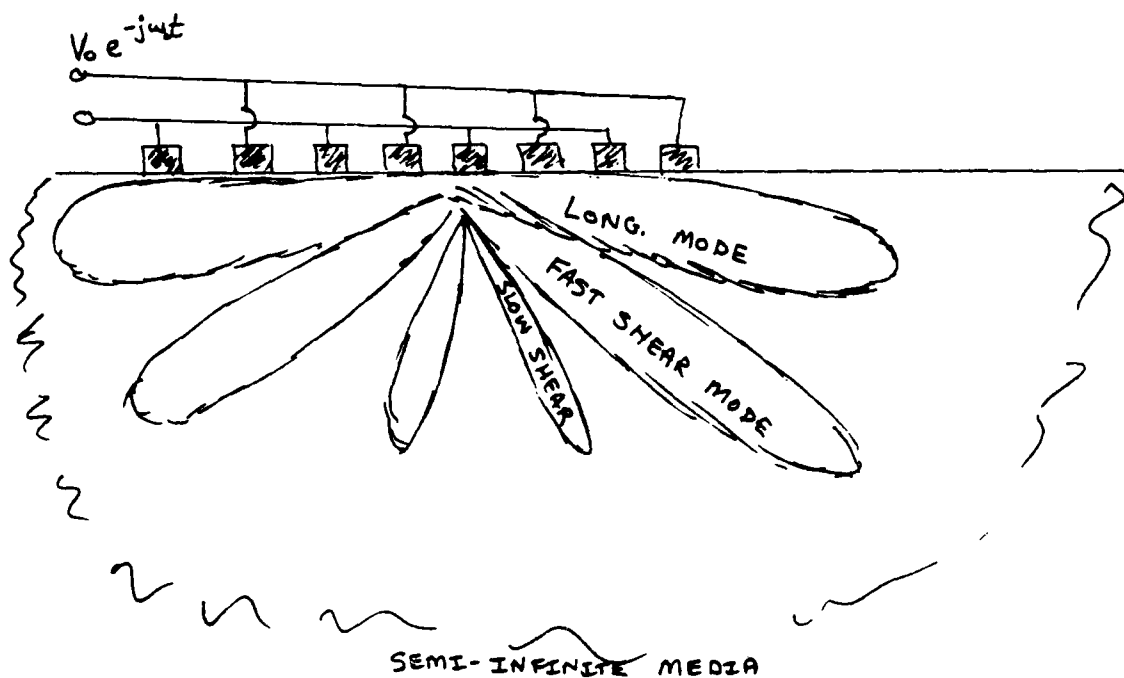region of the electrodes.

Figure **A.4.6** Transducer radiation Bulk waves at   , the
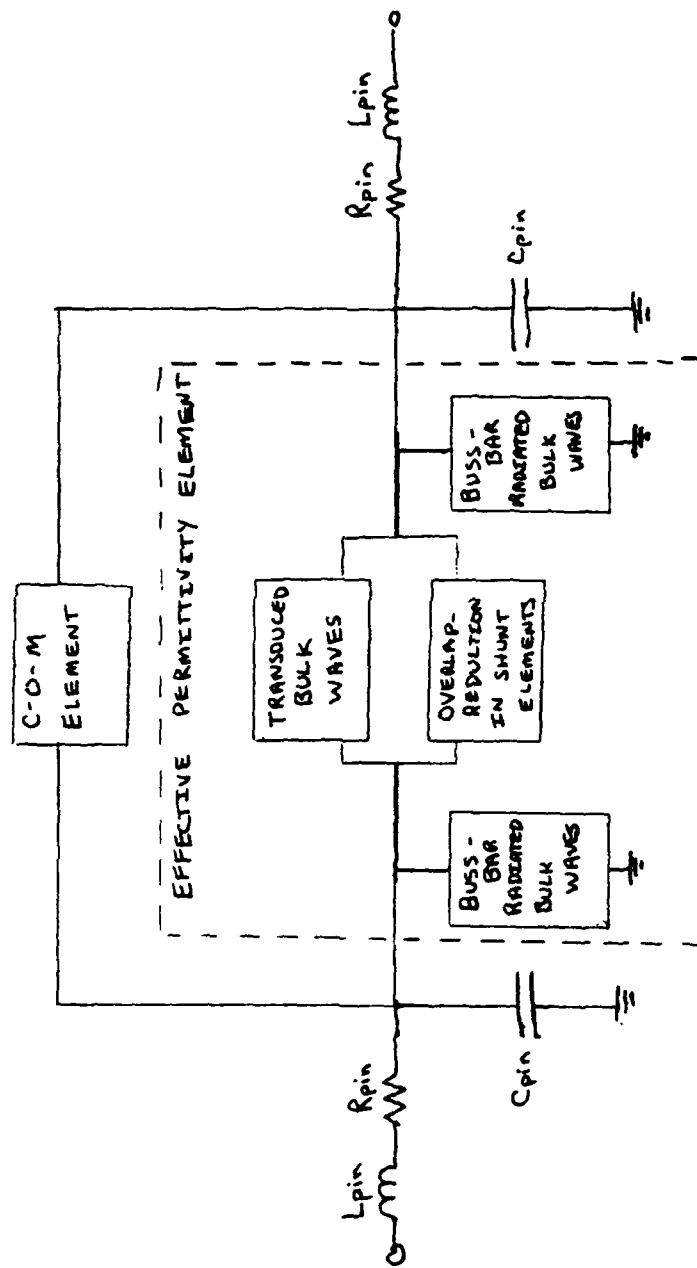longitudinal mode cut-off frequency.

Figure A5 Structure of the SNE model at the "Device" level, showing the "Effective Permittivity Element", The "Com Element" and Pin parasitics.

BIBLIOGRAPHY

(1) Ishihara, Koyomada, and Yoshikawa, "Narrow Band Filters Using SAW Resonators", 1975 IEEE Ultrasonics Symposium, pp 381-384.

(2) US Patent #4,599,587, "Impedance Element", C. S. Hartmann, RF Monolithics, July 8, 1986.

(3) A. L. Nalamwar and M. Epstein, "Immitance Characterization of Acoustic Surface Wave Transducers", Proc. IEEE (Lett.), v. 60, pp 336-337, Mar. 1972.

(4) US Patent #4,577,168, "Notch Filter", C. S. Hartmann, RF Monolithics, March 18, 1986.

(5) US Patent 4,599,587 (1986)

(6) Hartmann, Andle and King "SAW Notch Filters", 1987 IEEE Ultrasonics Symposium, Oct. 1987.

(7) Andle and King, "Novel Notch Elements Bring SAW Shaping To Filter Circuits," Microwaves & RF, Dec. 1987, pp.107-111.

(8) Nalamwar and Epstein, "Ommitance Characterization of Acoustic Surface Wave Transducers", Proc. IEEE (Lett.), v. 60, pp. 336-337, Mar. 1972.

(9) Hartmann and Wright, "An analysis of SAW Interdigital Transducers with Internal Reflections and the Application to the design of Single Phase Unidirectional Transducers," Proc. of 1982 IEEE Ultrasonics Symposium.

(10) Hartmann, "Impulse Model Design of Acoustic Surface Wave Filters," IEEE Transactions on Microwave Theory and Technique, Vol. MTT-21, (April 1973), pp.162-175.

(11) Vigil, Abbott and Malocha, "A Study of the Effects of Apodized Geometries on SAW Filter Parameters," 1987 IEEE Ultrasonics Symposium, Oct. 1987.

(12) Hartmann, "Weighting Interdigital Surface Wave Transducers by Selective Withdrawal of Electrodes", 1973 IEEE Ultrasonics Symposium, pp. 423-426.

(13) Wright, "The Natural Single Phase Unidirectional Transducer: A New Low-Loss SAW Transducer", Proc. 1985 IEEE Ultrasonics Symposium.

(14) US Patent No. 4,670,681 (1987)

(15) Wright, "Experimental and Theoretical Research on an Innovative Unidirectional Surface Acoustic Wave Transducer," Phase II Final Report for the National Science Foundation (Grant Number ECS-8116654.

(16) Milsom, Reilly and Redwood, "Analysis of Generation and Detection of Surface and Bulk Acoustic Waves by Interdigital Transducers," IEEE Trans. SU-24, pp. 147-166 (1971).

(17) Hartman, "Density of Thin Evaporated Aluminum Films," Journal of Vacuum Science and Technology Volume 2, Number 5, p.239, September/October, 1965.